Planet-Disc Interactions and Early Evolution of Planetary Systems

Clément Baruteau
University of Cambridge

Aurélien Crida
Universtité Nice Sophia Antipolis / Observatoire de la Côte d'Azur

Sijme-Jan Paardekooper
University of Cambridge

Frédéric Masset
Universidad Nacional Autónoma de México

Jérôme Guilet
University of Cambridge

Bertram Bitsch
Universtité Nice Sophia Antipolis / Observatoire de la Côte d'Azur

Richard Nelson
Queen Mary, University of London

Wilhelm Kley
Universität Tübingen

John Papaloizou
University of Cambridge

The great diversity of extrasolar planetary systems has challenged our understanding of how planets form, and how their orbits evolve as they form. Among the various processes that may account for this diversity, the gravitational interaction between planets and their parent protoplanetary disc plays a prominent role in shaping young planetary systems. Planet-disc forces are large, and the characteristic times for the evolution of planets orbital elements are much shorter than the lifetime of protoplanetary discs. The determination of such forces is challenging, because it involves many physical mechanisms and it requires a detailed knowledge of the disc structure. Yet, the intense research of the past few years, with the exploration of many new avenues, represents a very significant improvement on the state of the discipline. This chapter reviews current understanding of planet-disc interactions, and highlights their role in setting the properties and architecture of observed planetary systems.

1. INTRODUCTION

Since the fifth edition of Protostars and Planets in 2005 (PPV) the number of extrasolar planets has increased from about 200 to nearly 1000, with several thousand transiting planet candidates awaiting confirmation. These prolific discoveries have emphasized the amazing diversity of exoplanetary systems. They have brought crucial constraints on models of planet formation and evolution, which need to account for the many flavors in which exoplanets come. Some giant planets, widely known as the hot Jupiters, orbit their star in just a couple of days, like 51 Pegasus b (*Mayor and Queloz*, 1995). Some others orbit their star in few ten to hundred years, like the four planets known to date in the HR 8799 planetary system (*Marois et al.*, 2010). At the time of PPV, it was already established that exoplanets have a broad distribution of eccentricity, with a median value ≈ 0.3 (*Takeda and Rasio*, 2005). Since then, measurements

of the Rossiter McLaughlin effect in about 50 planetary systems have revealed several hot Jupiters on orbits highly misaligned with the equatorial plane of their star (e.g., *Albrecht et al.*, 2012), suggesting that exoplanets could also have a broad distribution of inclination. Not only should models of planet formation and evolution explain the most exotic flavors in which exoplanets come, they should also reproduce their statistical properties. This is challenging, because the predictions of such models depend sensitively on the many key processes that come into play. One of these key processes is the interaction of forming planets with their parent protoplanetary disc, which is the scope of this chapter.

Planet-disc interactions play a prominent role in the orbital evolution of young forming planets, leading to potentially large variations not only in their semi-major axis (a process known as planet migration), but also in their eccentricity and inclination. Observations (i) of hot Jupiters on orbits aligned with the equatorial plane of their star, (ii) of systems with several coplanar low-mass planets with short and intermediate orbital periods (like those discovered by the Kepler mission), (iii) and of many near-resonant multi-planet systems, are evidence that planet-disc interactions are one major ingredient in shaping the architecture of observed planetary systems. But, it is not the only ingredient: planet-planet and star-planet interactions are also needed to account for the diversity of exoplanetary systems. The long-term evolution of planetary systems after the dispersal of their protoplanetary disc is reviewed in the chapter by Davies et al.

This chapter commences with a general description of planet-disc interactions in section 2. Basic processes and recent progress are presented with the aim of letting non-experts pick up a physical intuition and a sense of the effects in planet-disc interactions. Section 3 continues with a discussion on the role played by planet-disc interactions in the properties and architecture of observed planetary systems. Summary points follow in section 4.

2. THEORY OF PLANET-DISC INTERACTIONS

2.1. Orbital evolution of low-mass planets: type I migration

Embedded planets interact with the surrounding disc mainly through gravity. Disc material, in orbit around the central star, feels a gravitational perturbation caused by the planet that can lead to an exchange of energy and angular momentum between planet and disc. In this section, we assume that the perturbations due to the planet are small, so that the disc structure does not change significantly due to the planet, and that migration is slow, so that any effects of the radial movement of the planet can be neglected. We will return to these issues in sections 2.2 and 2.3. If these assumptions are valid, we are in the regime of type I migration, and we are dealing with low-mass planets (typically up to Neptune's mass).

The perturbations in the disc induced by the planet are traditionally split into two parts: (i) a wave part, where the disc response comes in the form of spiral density waves propagating throughout the disc from the planet location, and (ii) a part confined in a narrow region around the planet's orbital radius, called the planet's horseshoe region, where disc material executes horseshoe turns relative to the planet. An illustration of both perturbations is given in Fig. 1. We will deal with each of them separately below. For simplicity, we will focus on a two-dimensional disc, characterised by vertically averaged quantities such as the surface density Σ. We make use of cylindrical polar coordinates (r, φ) centred on the star.

2.1.1. Wave torque

It has been known for a long time that a planet exerting a gravitational force on its parent disc can launch waves in the disc at Lindblad resonances (*Goldreich and Tremaine*, 1979, 1980). These correspond to locations where the gas azimuthal velocity relative to the planet matches the phase velocity of acoustic waves in the azimuthal direction. This phase velocity depends on the azimuthal wavenumber, the sound speed and the epicyclic frequency, that is the oscillation frequency of a particle in the disc subject to a small radial displacement (e.g., *Ward*, 1997). At large azimuthal wavenumber, the phase velocity tends to the sound speed, and Lindblad resonances therefore pile up at $r = a_{\rm p} \pm 2H/3$, where $a_{\rm p}$ is the semi-major axis of the planet and $H \ll r$ is the pressure scaleheight of the disc (*Artymowicz*, 1993b). The superposition of the waves launched at Lindblad resonances gives rise to a one-armed spiral density wave (*Ogilvie and Lubow*, 2002), called the wake (see Fig. 1).

It is possible to solve the wave excitation problem in the linear approximation and calculate analytically the resulting torque exerted on the disc using the WKB approximation (*Goldreich and Tremaine*, 1979; *Lin and Papaloizou*, 1979). Progress beyond analytical calculations for planets on circular orbits has been made by solving the linear perturbation equations numerically, as done in 2D in *Korycansky and Pollack* (1993). The three-dimensional case was tackled in *Tanaka et al.* (2002), which resulted in a widely used torque formula valid for isothermal discs only. It is important to note that 2D calculations only give comparable results to more realistic 3D calculations if the gravitational potential of the planet is softened appropriately. Typically, the softening length has to be a sizeable fraction of the disc scaleheight (*Müller et al.*, 2012). Using this 2D softened gravity approach, *Paardekooper et al.* (2010) found that the dependence of the wave torque[1] ($\Gamma_{\rm L}$) on disc gradients in a non-isothermal, adiabatic disc is

$$\gamma \Gamma_{\rm L}/\Gamma_0 = -2.5 - 1.7\beta + 0.1\alpha, \qquad (1)$$

where γ is the ratio of specific heats, α and β are negatives of the (local) power law exponents of the surface density Σ

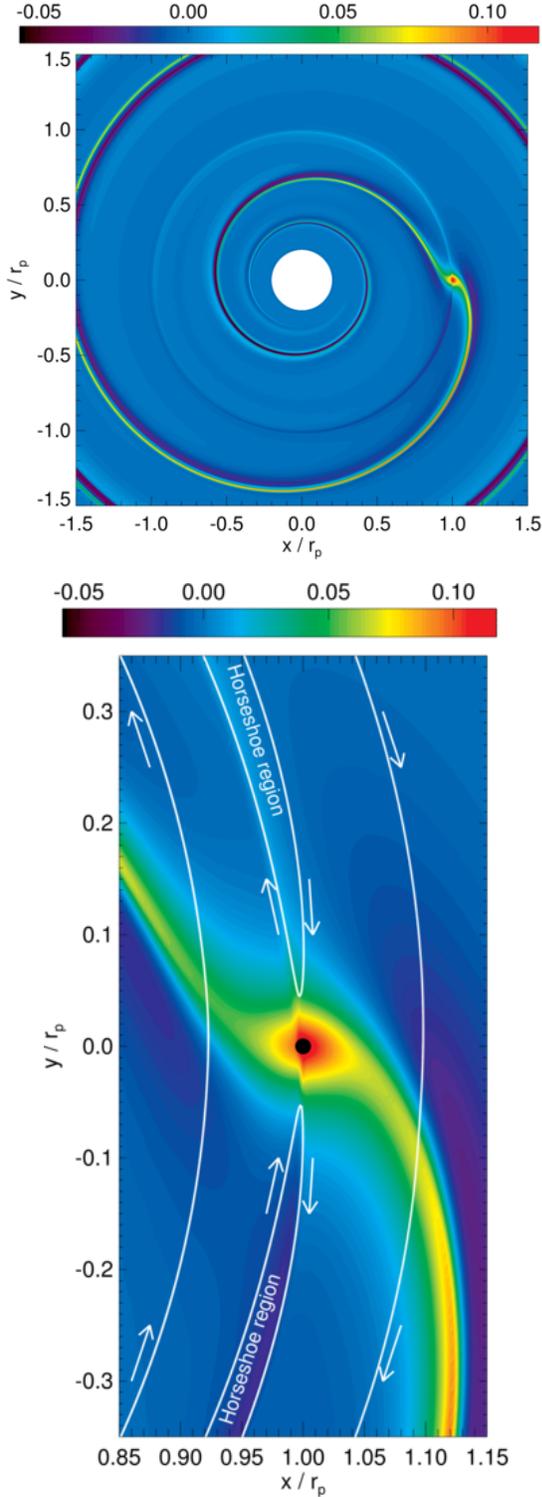[1] The wave torque exerted on the planet is also commonly referred to as the Lindblad torque.

Fig. 1.— Relative perturbation of the surface density of a gaseous protoplanetary disc perturbed by a 5 Earth-mass planet located at $x = r_p$ and $y = 0$. The planet induces a one-armed spiral density wave – the *wake* – that propagates throughout the disc, and density perturbations confined in the planet's horseshoe region. Typical gas trajectories relative to the planet are shown with white curves and arrows in the bottom panel.

and temperature T ($\Sigma \propto r^{-\alpha}$, $T \propto r^{-\beta}$), and the torque is normalised by

$$\Gamma_0 = \frac{q^2}{h^2} \Sigma_p r_p^4 \Omega_p^2, \qquad (2)$$

where q is the planet-to-star mass ratio, $h = H/r$ is the aspect ratio and quantities with subscript p refer to the location of the planet. Note that in general we expect $\alpha, \beta > 0$, i.e. both surface density and temperature decrease outward. For reasonable values of α, the wave torque on the planet is negative: it decreases the orbital angular momentum of the planet, and thus its semi-major axis (the planet being on a circular orbit), leading to inward migration. The linear approximation remains valid as long as $q \ll h^3$ (*Korycansky and Papaloizou*, 1996). For a disc around a Solar mass star with $h = 0.05$ this means that the planet mass needs to be much smaller than $40 \, M_{\oplus}$.

The factor γ in Eq. (1) is due to the difference in sound speed between isothermal and adiabatic discs (*Baruteau and Masset*, 2008a). For discs that can cool efficiently, we expect the isothermal result to be valid ($\gamma \rightarrow 1$), while for discs that can not cool efficiently, the adiabatic result should hold. It is possible to define an effective γ that depends on the thermal diffusion coefficient so that the isothermal regime can be connected smoothly to the adiabatic regime (*Paardekooper et al.*, 2011).

A generalized expression for the Lindblad torque has been derived by *Masset* (2011) for 2D discs where the density and temperature profiles near the planet are not power laws, like at opacity transitions or near cavities. This generalized expression agrees well with Eq. (1) for power-law discs. We stress that there is to date no general expression for the wave torque in 3D non-isothermal discs. The analytics is involved (*Tanaka et al.*, 2002; *D'Angelo and Lubow*, 2010) and it is difficult to measure the wave torque independently from the corotation torque in 3D numerical simulations of planet-disc interactions.

The above discussion neglected possible effects of self-gravity. *Pierens and Huré* (2005) showed that in a self-gravitating disc, Lindblad resonances get shifted towards the planet, thereby making the wave torque stronger. This was confirmed numerically by *Baruteau and Masset* (2008b). The impact of a magnetic field in the disc and of possibly related MHD turbulence will be considered in Section 2.1.4.

The normalisation factor Γ_0 sets a time scale for Type I migration of planets on circular orbits:

$$\tau_0 = \frac{r_p}{|dr_p/dt|} = \frac{1}{2} \frac{h^2}{q} \frac{M_\star}{\Sigma_p r_p^2} \Omega_p^{-1}, \qquad (3)$$

where $M_\star$ denotes the mass of the central star. Assuming a typical gas surface density of $2000 \, (r_p/1 \, \text{AU})^{-3/2} \, \text{g cm}^{-2}$, $M_\star = M_\odot$, and $h = 0.05$, the migration time scale in years at 1 Astronomical Unit (AU) is given approximately by $1/q$. This means that an Earth-mass planet at 1 AU would migrate inward on a time scale of $\sim 3 \times 10^5$ years, while the time scale for Neptune would only be $\sim 2 \times 10^4$ years. All

these time scales are shorter than the expected disc life time of $10^6 - 10^7$ years, making this type of migration far too efficient for planets to survive on orbits of several AU. A lot of work has been done recently on how to stop Type I migration or make it less efficient (see sections 2.1.2 and 2.1.3).

2.1.2. Corotation torque

Most progress since PPV (*Papaloizou et al.*, 2007) has been made in understanding the torque due to disc material that on average corotates with the planet, the corotation torque. It is possible, by solving the linearised disc equations in the same way as for the wave torque, to obtain a numerical value for the corotation torque. One can show that in the case of an isothermal disc, this torque scales with the local gradient in specific vorticity or vortensity[2] (*Goldreich and Tremaine*, 1979). It therefore has a stronger dependence on background surface density gradients than the wave torque, with shallower profiles giving rise to a more positive torque. It was nevertheless found in *Tanaka et al.* (2002) that, except for extreme surface density profiles, the wave torque always dominates over the linear corotation torque ($\Gamma_{c,lin}$). *Paardekooper et al.* (2010) obtained, in the 2D softened gravity approach, for a non-isothermal disc

$$\gamma \Gamma_{c,lin}/\Gamma_0 = 0.7\left(\frac{3}{2} - \alpha - \frac{2\xi}{\gamma}\right) + 2.2\xi, \qquad (4)$$

where $\xi = \beta - (\gamma - 1)\alpha$ is the negative of the (local) power law exponent of the specific entropy. For an isothermal disc, $\xi = 0$ and the corotation torque is proportional to the vortensity gradient.

An alternative expression for the corotation torque was derived by *Ward* (1991) by considering disc material on horseshoe orbits relative to the planet. This disc material defines the planet's horseshoe region (see bottom panel in Fig. 1). The torque on the planet due to disc material executing horseshoe turns, the horseshoe drag, scales with the vortensity gradient in an isothermal disc, just like the linear corotation torque. It comes about because material in an isothermal inviscid fluid conserves its vortensity. When executing a horseshoe turn, which takes a fluid element to a region of different vorticity because of the Keplerian shear, conservation of vortensity dictates that the surface density should change (*Ward*, 1991). In a gas disc, this change in surface density is smoothed out by evanescent pressure waves (*Casoli and Masset*, 2009). Nevertheless, this change in surface density results in a torque being applied on the planet.

For low-mass planets, for which $q \ll h^3$, the half-width of the horseshoe region, x_s, is (*Masset et al.*, 2006; *Paardekooper and Papaloizou*, 2009b)

$$x_s \approx 1.2 r_p \sqrt{q/h}. \qquad (5)$$

[2]Vorticity is defined here as the vertical component of the curl of the gas velocity. In a 2D disc model, specific vorticity, or vortensity, refer to vorticity divided by surface density.

Thus it is only a fraction of the local disc thickness. The horseshoe drag, which scales as x_s^4 (*Ward*, 1991), therefore has the same dependence on q and h as the wave torque and the linear corotation torque. The numerical coefficient in front is generally much larger than for the linear corotation torque, however (*Paardekooper and Papaloizou*, 2009a; *Paardekooper et al.*, 2010). Since both approaches aim at describing the same thing, *the* corotation torque, it was long unclear which result to use. It was shown in *Paardekooper and Papaloizou* (2009a) that whenever horseshoe turns occur, the linear corotation torque gets replaced by the horseshoe drag, unless a sufficiently strong viscosity is applied. It should be noted that horseshoe turns do not exist within linear theory, making linear theory essentially invalid for low-mass planets as far as the corotation torque is concerned.

The corotation torque in the form of horseshoe drag is very sensitive to the disc's viscosity and thermal properties near the planet. *Paardekooper and Mellema* (2006) found that in 3D radiation hydrodynamical simulations, migration can in fact be directed *outwards* due to a strong positive corotation torque counterbalancing the negative wave torque over the short duration (15 planet orbits) of their calculations. This was subsequently interpreted as being due to a radial gradient in disc specific entropy, which gives rise to a new horseshoe drag component due to conservation of entropy in an adiabatic disc (*Baruteau and Masset*, 2008a; *Paardekooper and Mellema*, 2008; *Paardekooper and Papaloizou*, 2008). The situation is, however, not as simple as for the isothermal case. It turns out that the entropy-related horseshoe drag arises from the production of vorticity along the downstream separatrices of the planet's horseshoe region (*Masset and Casoli*, 2009). Conservation of entropy during a horseshoe turn leads to a jump in entropy along the separatrices whenever there is a radial gradient of entropy in the disc. This jump in entropy acts as a source of vorticity, which in turn leads to a torque on the planet. Crucially, the amount of vorticity produced depends on the streamline topology, in particular the distance of the stagnation point to the planet. An analytical model for an adiabatic disc where the background temperature is constant was developed in *Masset and Casoli* (2009), while *Paardekooper et al.* (2010) used a combination of physical arguments and numerical results to obtain the following expression for the horseshoe drag:

$$\gamma \Gamma_{c,HS}/\Gamma_0 = 1.1\left(\frac{3}{2} - \alpha\right) + 7.9\frac{\xi}{\gamma}, \qquad (6)$$

where the first term on the right hand side is the vortensity-related part of the horseshoe drag, and the second term is the entropy-related part. The model derived in *Masset and Casoli* (2009), under the same assumptions for the stagnation point, yields a numerical coefficient for the entropy-related part of the horseshoe drag of 7.0 instead of 7.9.

Comparing the linear corotation torque to the non-linear horseshoe drag – see Eqs. (4) and (6) – we see that both depend on surface density and entropy gradients, but also that

the horseshoe drag is always stronger. In the inner regions of discs primarily heated by viscous heating, the entropy profile should decrease outward ($\xi > 0$). The corotation torque should then be positive, promoting outward migration.

The results presented above were for adiabatic discs, while the isothermal result can be recovered by setting $\gamma = 1$ and $\beta = 0$ (which makes $\xi = 0$ as well). Real discs are neither isothermal nor adiabatic. When the disc can cool efficiently, which happens in the optically thin outer parts, the isothermal result is expected to be valid (or rather the *locally* isothermal result: a disc with a fixed temperature profile, which behaves slightly differently from a truly isothermal disc; see *Casoli and Masset*, 2009). In the optically thick inner parts of the disc, cooling is not efficient and the adiabatic result should hold. An interpolation between the two regimes was presented in *Paardekooper et al.* (2011) and *Masset and Casoli* (2010).

2.1.3. Saturation of the corotation torque

While density waves transport angular momentum away from the planet, the horseshoe region only has a finite amount of angular momentum to play with since there are no waves involved. Sustaining the corotation torque therefore requires a flow of angular momentum into the horseshoe region: unlike the wave torque, the corotation torque is prone to *saturation*. In simulations of disc-planet interactions, sustaining (or unsaturating) the corotation torque is usually established by including a Navier-Stokes viscosity. In a real disc, angular momentum transport is likely due to turbulence arising from the magneto-rotational instability (MRI; see chapter by Turner et al.), and simulations of turbulent discs give comparable results to viscous discs (*Baruteau and Lin*, 2010; *Baruteau et al.*, 2011a; *Pierens et al.*, 2012) as far as saturation is concerned (see also Section 2.1.4). The main result for viscous discs is that the viscous diffusion time scale across the horseshoe region has to be shorter than the libration time scale in order for the horseshoe drag to be unsaturated (*Masset*, 2001, 2002). This also holds for non-isothermal discs, and expressions for the corotation torque have been derived in 2D disc models for general levels of viscosity and thermal diffusion or cooling (*Masset and Casoli*, 2010; *Paardekooper et al.*, 2011). Results from 2D radiation hydrodynamic simulations, where the disc is self-consistently heated by viscous dissipation and cooled by radiative losses, confirm this picture (*Kley and Crida*, 2008).

The torque expressions of *Masset and Casoli* (2010) and *Paardekooper et al.* (2011) were derived using 2D disc models, and 3D disc models are still required to get definitive, accurate predictions for the wave and the corotation torques. Still, the predictions of the aforementioned torque expressions are in decent agreement with the results of 3D simulations of planet-disc interactions. The simulations of *D'Angelo and Lubow* (2010) explored the dependence of the total torque with density and temperature gradients in 3D locally isothermal discs. They found the total normalized torque $\Gamma_{\mathrm{tot}}/\Gamma_0 \approx -1.4 - 0.4\beta - 0.6\alpha$. For the planet mass and disc viscosity of these authors, the corotation torque reduces to the linear corotation torque. Summing Eqs. (1) and (4) with $\gamma = 1$ and $\xi = \beta$ yields $\Gamma_{\mathrm{tot}}/\Gamma_0 = -1.4 - 0.9\beta - 0.6\alpha$, which is in good agreement with the results of *D'Angelo and Lubow* (2010), except for the coefficient in front of the temperature gradient. The simulations of *Kley et al.* (2009), *Ayliffe and Bate* (2011) and *Bitsch and Kley* (2011) were for non-isothermal radiative discs. *Ayliffe and Bate* (2011) considered various temperature power-law profiles and showed that the total torque does not always exhibit a linear dependence with temperature gradient. *Bitsch and Kley* (2011) highlighted substantial discrepancies between the torque predictions of *Masset and Casoli* (2010) and *Paardekooper et al.* (2011). These discrepancies originate from a larger half-width (x_{s}) of the planet's horseshoe region adopted in *Masset and Casoli* (2010), which was suggested as a proxy to assess the corotation torque in 3D. Adopting the same, standard value for x_{s} given by Eq. (5), one can show that the total torques of *Masset and Casoli* (2010) and *Paardekooper et al.* (2011) are actually in very good agreement. Both are less positive than in the numerical results of *Bitsch and Kley* (2011). Discrepancies originate from inherent torque differences between 2D and 3D disc models (see, e.g., *Kley et al.*, 2009), and possibly from a non-linear boost of the positive corotation torque in the simulations of *Bitsch and Kley* (2011), for which $q \gtrsim h^3$ (for locally isothermal discs, see *Masset et al.*, 2006).

The thermal structure of protoplanetary discs is determined not only by viscous heating and radiative cooling, but also by stellar irradiation. The effects of stellar irradiation on the disc structure have been widely investigated using a 1+1D numerical approach (e.g., *Bell et al.*, 1997; *Dullemond et al.*, 2001), with the goal to fit the spectral energy distributions of observed discs. Stellar heating dominates in the outer regions of discs, viscous heating in the inner regions. The disc's aspect ratio should then slowly increase with increasing distance from the star (*Chiang and Goldreich*, 1997). This increase may have important implications for the direction and speed of type I migration which, as we have seen above, are quite sensitive to the aspect ratio (local value and radial profile). This is illustrated in Fig. 2, which displays the torque acting on type I migrating planets sitting in the midplane of their disc, with and without inclusion of stellar irradiation. The disc structure was calculated in *Bitsch et al.* (2013b) for standard opacities and a constant disc viscosity (thereby fixing the density profile). Two regions of outward migration originate from opacity transitions at the silicate condensation line (near 0.8 AU) and at the water ice line (near 5 AU). In this model, heating by stellar irradiation becomes prominent beyond ≈ 8 AU. The resulting increase in the disc's aspect ratio profile gives a shallower entropy profile (β and thus ξ take smaller values) and therefore a smaller (though positive) entropy-related horseshoe drag – see Eq. (6). Inclusion of stellar ir-
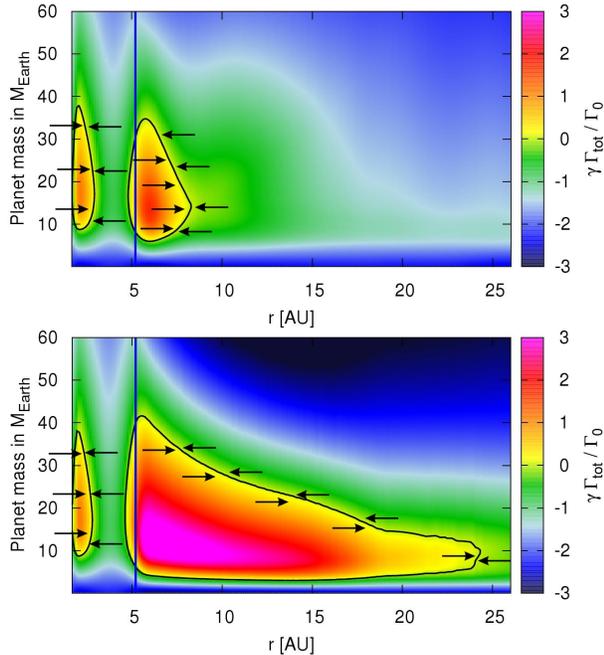
Fig. 2.— Type I migration torque on planets of different masses in disc models with stellar irradiation (top) and without (bottom). The torque expressions in *Paardekooper et al.* (2011) are used and expressed in units of Γ_0, given by Eq. (2). Black lines delimit areas where migration is directed outward. Black arrows show the direction of migration, and the blue line the ice line location at 170K. Adapted from *Bitsch et al.* (2013b).

radiation therefore reduces the range of orbital separations at which outward migration may occur (see also *Kretke and Lin*, 2012). The outer edge of regions of outward migration are locations where type I planetary cores converge, which may lead to resonant captures (*Cossou et al.*, 2013) and could enhance planet growth if enough cores are present to overcome the trapping process. Note in Fig. 2 that planets up to $\sim 5 M_\oplus$ do not migrate outwards. This is because for such planet masses, and for the disc viscosity in this model ($\alpha_\nu \sim$ a few $\times 10^{-3}$), the corotation torque is replaced by the (smaller) linear corotation torque.

Fig. 2 provides a good example of how sensitive predictions of planet migration models can be to the structure of protoplanetary discs. Future observations of discs, for example with ALMA, will give precious information that will help constrain migration models.

2.1.4. Effect of disc magnetic field and turbulence

So far we have considered the migration of a planet in a purely hydrodynamical laminar disc where turbulence is modelled by an effective viscosity. As stressed in Section 2.1.2, a turbulent viscosity is essential to unsaturate the corotation torque. The most likely (and best studied) source of turbulence in protoplanetary discs is the Magneto-Rotational Instability (MRI; *Balbus and Hawley*, 1991) which can amplify the magnetic field and drive MHD turbulence by tapping energy from the Keplerian shear. Further-

more, the powerful jets observed to be launched from proto-planetary discs are thought to arise from a strong magnetic field (likely through the magneto-centrifugal acceleration; see *Ferreira et al.*, 2006). Magnetic field and turbulence thus play a crucial role in the dynamics and evolution of protoplanetary discs, and need to be taken into account in theories of planet-disc interactions.

Stochastic torque driven by turbulence. MHD turbulence excites non-axisymmetric density waves (see left panel in Fig. 3) which cause a fluctuating component of the torque on a planet in a turbulent disc (*Nelson and Papaloizou*, 2004; *Nelson*, 2005; *Laughlin et al.*, 2004). This torque changes sign stochastically with a typical correlation time of a fraction of an orbit. Because the density perturbations are driven by turbulence rather than the planet itself, the specific torque due to turbulence is independent of planet mass, while the (time-averaged) specific torque driving type I migration is proportional to the planet mass. Type I migration should therefore outweigh the stochastic torque for sufficiently massive planets and on a long-term evolution, whereas stochastic migration arising from turbulence should dominate the evolution of planetesimals and possibly small mass planetary cores (*Baruteau and Lin*, 2010; *Nelson and Gressel*, 2010). The stochastic torque adds a random walk component to planet migration, which can be represented in a statistical sense by a diffusion process acting on the probability distribution of planets (*Johnson et al.*, 2006; *Adams and Bloch*, 2009). A consequence of this is that a small fraction of planets may migrate to the outer parts of their disc even if the laminar type I migration is directed inwards. Note that the presence of a dead zone around the disc's midplane, where MHD turbulence is quenched due the low ionization, reduces the amplitude of the stochastic torque (*Oishi et al.*, 2007; *Gressel et al.*, 2011, 2012).

Mean migration in a turbulent disc. 2D hydrodynamical simulations of discs with stochastically forced waves have been carried out to mimic MHD turbulence and to study its effects on planet migration. Using *Laughlin et al.* (2004)'s model, *Baruteau and Lin* (2010) and *Pierens et al.* (2012) showed that, when averaged over a sufficiently long time, the torque converges toward a well-defined average value, and that the effects of turbulence on this average torque are well described by an effective turbulent viscosity and heat diffusion. In particular, the wave torque is little affected by turbulence, while the corotation torque can be unsaturated by this wake-like turbulence. *Baruteau et al.* (2011a) and *Uribe et al.* (2011) have shown that a similar conclusion holds in simulations with fully developed MHD turbulence arising from the MRI. *Baruteau et al.* (2011a) however discovered the presence of an additional component of the corotation torque, which has been attributed to the effect of the magnetic field (*Guilet et al.*, 2013, see below). Note that the mean migration in a turbulent disc has been conclusively studied only for fairly massive planets (typically $q/h^3 \sim 0.3$) as less massive planets need a better resolution and a longer averaging time. It is an open question whether
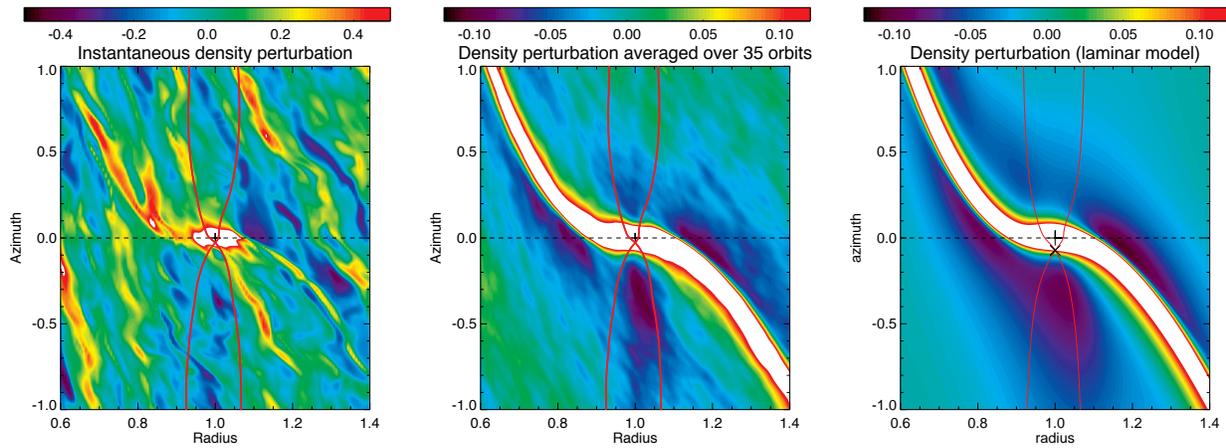
Fig. 3.— Surface density perturbation of a 3D MRI-turbulent disc with a planet embedded at $r = 1$ and $\varphi = 0$ (left and middle panels; adapted from *Baruteau et al.*, 2011a) and in an equivalent 2D laminar disc with an azimuthal magnetic field (right panel, adapted from *Guilet et al.*, 2013). In the turbulent simulation, the planet wake is barely visible in the instantaneous density perturbation (left), because of the large turbulent density fluctuations. When averaged over 35 orbits, density perturbations agree very well with those of the equivalent laminar disc model (compare the middle and right panels), revealing not only the planet wake, but also an asymmetric under-density confined in the planet's horseshoe region and arising from the azimuthal magnetic field. The separatrices of the planet's horseshoe region are shown by red curves.

the migration of smaller planets is affected by turbulence in a similar way as by a diffusion process. One may wonder indeed whether the diffusion approximation remains valid when the width of the planet's horseshoe region is a small fraction of the disc scaleheight and therefore of the typical correlation length of turbulence.

Wave torque with a magnetic field. In addition to driving turbulence, the magnetic field has a direct effect on planet migration by modifying the response of the gas to the planet's potential. In particular, waves propagation is modified by the magnetic field and three types of waves exist: fast and slow magneto-sonic waves as well as Alfvén waves. *Terquem* (2003) showed that for a strong azimuthal magnetic field, slow MHD waves are launched at the so-called magnetic resonances, which are located where the gas azimuthal velocity relative to the planet matches the phase velocity of slow MHD waves. The angular momentum carried by the slow MHD waves gives rise to a new component of the torque. If the magnetic field strength is steeply decreasing outwards, this new torque is positive and may lead to outward migration (*Terquem*, 2003; *Fromang et al.*, 2005). A vertical magnetic field also impacts the resonances (*Muto et al.*, 2008) but its effect on the total torque remains to be established. In the inner parts of protoplanetary discs, the presence of a strong vertical magnetic field is needed to explain the launching of observed jets. A better understanding of the strength and evolution of such a vertical field (*Guilet and Ogilvie*, 2012, 2013) and of its effect on planet migration will improve the description of planet migration near the central star.

Corotation torque with a magnetic field. A strong azimuthal magnetic field can prevent horseshoe motions so that the corotation torque is replaced by the torque aris-

ing from magnetic resonances as discussed in the previous paragraph. *Guilet et al.* (2013) showed that horseshoe motions take place and suppress magnetic resonances for weak enough magnetic fields, when the Alfvén speed is less than the shear velocity at the separatrices of the planet's horseshoe region. Using 2D laminar simulations with effective viscosity and resistivity, these authors showed that advection of the azimuthal magnetic field along horseshoe trajectories leads to an accumulation of magnetic field near the downstream separatrices of the horseshoe region. This accumulation in turns leads to an under-density at the same location to ensure approximate pressure balance (see right panel in Fig. 3). The results of these laminar simulations agree very well with those of the MHD turbulent simulations of *Baruteau et al.* (2011a). A rear-front asymmetry in the magnetic field accumulation inside the horseshoe region gives rise to a new component of the corotation torque, which may cause outward migration even if the magnetic pressure is less than one percent of the thermal pressure (*Guilet et al.*, 2013). This new magnetic corotation torque could take over the entropy-related corotation torque to sustain outward migration in the radiatively efficient outer parts of protoplanetary discs. Future studies should address the behaviour of the corotation torque in the dead zone, and in regions of the disc threaded by a vertical magnetic field. Also, other non-ideal MHD effects, such as the Hall effect and ambipolar diffusion, can have a significant impact on the MRI turbulence and on the disc structure (e.g., *Bai and Stone*, 2011; *Kunz and Lesur*, 2013; *Simon et al.*, 2013). These non-ideal MHD effects still need to be explored in the context of planet-disc interactions.

2.1.5. Evolution of eccentric or inclined low-mass planets

We have so far considered planet-disc interactions for low-mass planets on circular orbits. Interaction between two or more planets migrating in their parent disc may increase eccentricities (e) and inclinations (i) – see section 2.4. We examine below the orbital evolution of protoplanets on eccentric or inclined orbits due to planet-disc interactions.

In the limit of small eccentricities, it can be shown that the effect of the disc is to damp the eccentricity of type I migrating planets (*Goldreich and Tremaine*, 1980; *Artymowicz*, 1993a; *Masset*, 2008). Similar arguments can be made for inclined low-mass planets, for which planet-disc interactions damp the inclination in time (*Tanaka and Ward*, 2004). *Papaloizou and Larwood* (2000) have provided an analytic expression for the eccentricity damping time scale in 2D, while *Tanaka and Ward* (2004) derived expressions for the eccentricity and inclination damping time scales in 3D:

$$\tau_e = \frac{e}{|de/dt|} \approx 2.6\, h^2\, \tau_0, \quad \tau_i = \frac{i}{|di/dt|} \approx 3.7\, h^2\, \tau_0, \quad (7)$$

where τ_0 is given by Eq. (3). Note that, h^2 being very small, damping of e and i is much faster than migration. A single low-mass planet should therefore migrate on a circular and coplanar orbit. The above results were confirmed by hydrodynamical simulations (*Cresswell et al.*, 2007; *Bitsch and Kley*, 2010, 2011). Eccentricity and inclination damping rates can be alternatively derived using a dynamical friction formalism (*Muto et al.*, 2011; *Rein*, 2012b).

We have stressed above that the migration of low-mass planets can be directed outwards if the disc material in the horseshoe region exerts a strong positive corotation torque on the planet. Numerical simulations by *Bitsch and Kley* (2010) have shown that for small eccentricities, the magnitude of the corotation torque decreases with increasing eccentricity, which restricts the possibility of outward migration to planets with eccentricities below a few percent. A consequence of this restriction is to shift regions of convergent migration to smaller radii for mildly eccentric low-mass planets (see last two paragraphs in section 2.1.2, and *Cossou et al.*, 2013). In a very recent study, *Fendyke and Nelson* (2014) have explored in detail the influence of orbital eccentricity on the corotation torque for a range of disc and planet parameters. Their study indicates that the reason why the corotation torque decreases with increasing e is because the width of the horseshoe region narrows as e increases. Furthermore, by fitting the results from their suite of simulations with an analytic function, they find that the corotation torque scales with eccentricity according to the expression $\Gamma_c(e) = \Gamma_c(0)\exp\left(-e/e_f\right)$, where $\Gamma_c(e)$ is the corotation torque at eccentricity e, $\Gamma_c(0)$ that at zero eccentricity, and e_f is an e-folding eccentricity that scales linearly with the disc aspect ratio at the planet's orbital radius (the expression $e_f = h/2+0.01$ provides a good overall fit to the simulations). Furthermore, the Lindblad torque becomes more positive with increasing e (*Papaloizou and Larwood*,

2000). This sign reversal does not necessarily lead to outward migration as the torque on an eccentric planet changes both the planet's semi-major axis and eccentricity (see, e.g., *Masset*, 2008).

Orbital migration also changes when a low-mass planet acquires some inclination. The larger the inclination, the less time the planet interacts with the dense gas near the disc midplane, the smaller the corotation torque and the migration rate. Thus, inclined low-mass planets can only undergo outward migration if their inclination remains below a few degrees (*Bitsch and Kley*, 2011).

2.2. Orbital evolution of massive, gap-opening planets: type II migration

2.2.1. Gap opening

The wave torque described in section 2.1.1 is the sum of a positive torque exerted on the planet by its inner wake, and a negative torque exerted by its outer wake. Equivalently, the planet gives angular momentum to the outer disc (the disc beyond the planet's orbital radius), and it takes some from the inner disc. If the torque exerted by the planet on the disc is larger in absolute value than the viscous torque responsible for disc spreading, an annular gap is carved around the planet's orbit (*Lin and Papaloizou*, 1986a). In this simple one-dimensional picture, the gap width is the distance from the planet where the planet torque and the viscous torque balance each other (*Varnière et al.*, 2004). However, *Crida et al.* (2006) showed that the disc material near the planet also feels a pressure torque that comes about because of the non-axisymmetric density perturbations induced by the planet. In a steady state, the torques due to pressure, viscosity and the planet balance all together, and such condition determine the gap profile. The half-width of a planetary gap hardly exceeds about twice the size of the planet's Hill radius, defined as $r_{\rm H} = r_{\rm p}(q/3)^{1/3}$. A gap should therefore be understood as a narrow depleted annulus between an inner disc and an outer disc. The width of the gap carved by a Jupiter-mass planet does not exceed about 30% of the star-planet orbital separation.

Based on a semi-analytic study of the above torque balance, *Crida et al.* (2006) showed that a planet opens a gap with bottom density less than 10% of the background density if the dimensionless quantity $\mathcal{P}$ defined as

$$\mathcal{P} = \frac{3}{4}\frac{H}{r_{\rm H}} + \frac{50}{q\mathcal{R}} \quad (8)$$

is $\lesssim 1$. In Eq. (8), $\mathcal{R} = r_{\rm p}^2\Omega_{\rm p}/\nu$ is the Reynolds number, ν the disc's kinematic viscosity. Adopting the widely used alpha prescription for the disc viscosity, $\nu = \alpha_\nu H^2\Omega$, the above gap-opening criterion becomes

$$\frac{h}{q^{1/3}} + \frac{50\alpha_\nu h^2}{q} \lesssim 1. \quad (9)$$

This criterion is essentially confirmed by simulations of MRI-turbulent discs, although the width and depth of the

gap can be somewhat different from an equivalent viscous disc model (*Papaloizou et al.*, 2004; *Zhu et al.*, 2013).

We point out that Eq. (8) with $\mathcal{P} = 1$ can be solved analytically: the minimum planet-to-star mass ratio for opening a deep gap as defined above is given by

$$q_{\min} = \frac{100}{\mathcal{R}} \left[(X+1)^{1/3} - (X-1)^{1/3} \right]^{-3}, \qquad (10)$$

with $X = \sqrt{1 + 3\mathcal{R}h^3/800}$, and where above quantities are to be evaluated at the planet's orbital radius. Taking a Sun-like star, Eq. (10) shows that in the inner regions of protoplanetary discs, where typically $h = 0.05$ and $\alpha_\nu \sim$ a few $\times 10^{-3}$, planets with a mass on the order of that of Jupiter, or larger, will open a deep gap. In the dead zone of a protoplanetary disc, where α_ν can be one or two orders of magnitude smaller, planet masses $\gtrsim 50 M_\oplus$ will open a gap. At larger radii, where planets could form by gravitational instability, h is probably near 0.1, $\alpha_\nu \sim 10^{-2}$, and only planets above 10 Jupiter masses could open a gap (but, see section 3.2).

Eqs. (9) and (10) give an estimate of the minimum planet-to-star mass ratio for which a gap with density contrast $\gtrsim 90\%$ is carved. Recent simulations by *Duffell and MacFadyen* (2013) indicate that similarly deep gaps could be opened for mass ratios smaller than given by these equations in discs with very low viscosities, such as what is expected in dead zones. Note also that planets such that $\mathcal{P}$ is a few can open a gap with a density contrast of few tens of percent. This may concern planets of few Earth to Neptune masses in dead zones (e.g., *Rafikov*, 2002; *Muto et al.*, 2010; *Dong et al.*, 2011).

2.2.2. Type II migration

The formation of an annular gap around a planet splits the protoplanetary disc into an inner disc and an outer disc, which both repel the planet towards the centre of the gap. While the planet is locked in its gap, it continues to migrate as the disc accretes onto the star. Said differently, the planet follows the migration trajectory imposed by the disc (*Lin and Papaloizou*, 1986b), and the migration timescale is then the viscous accretion time, $\tau_\nu = r_p^2/\nu$. However, if the planet is much more massive than the gas outside the gap, the planet will slow down the disc viscous accretion. This occurs if $M_p > 4\pi \Sigma_o r_p^2$, where Σ_o is the surface density of the outer disc just outside the gap. When this occurs, the inner disc still accretes onto the star, while the outer disc is held by the planet. This leads to the partial (or total) depletion of the inner disc (see below). The migration timescale, which is then set by the balance between the viscous torque and the planet's inertia, is given by $\tau_\nu \times (M_p/4\pi \Sigma_o r_p^2)$.

The above considerations show that the timescale for type II migration (τ_{II}) is given by

$$\tau_{\mathrm{II}} = \tau_\nu \times \max \left(1, \frac{M_p}{4\pi \Sigma_o r_p^2} \right). \qquad (11)$$

Eq. (11) applies when a planet carves a deep gap, that is when $\mathcal{P} < 1$. However, when $\mathcal{P} \gtrsim 1.5$ and the density in-

side the gap exceeds about 20% of the background density, the planet and the gas are no longer decoupled. The gas in the gap exerts a corotation torque on the planet, which is usually positive. Therefore, the migration of planets that marginally satisfy the gap-opening criterion can be slower than in the standard type II migration. In particular, if the gap density is large enough, and depending on the local density and temperature gradients, the corotation torque can overcome the viscous torque and lead to outward migration (*Crida and Morbidelli*, 2007). Note that the drift of the planet relative to the gas may lead to a positive feedback on migration (see section 2.3).

2.2.3. Link with observations

Recently, gap structures similar to what are predicted by planet-disc interactions have been observed in the discs around HD169142 (*Quanz et al.*, 2013) and TW Hya (*Debes et al.*, 2013). The gap around HD169142 is located ~ 50 AU from the star, and seems to be quite deep (the surface brightness at the gap location is decreased by ~ 10). The gap around TW Hya is located ~ 80 AU from the star, and is much shallower (the decrease in surface brightness is only 30%). If confirmed, these would be the first observations of gaps in protoplanetary discs that could be carved by a planet.

Cavities have been observed in several circumstellar discs in the past few years. Contrary to a gap, a cavity is characterised by the absence of an inner disc. In each of these transition discs, observations indicate a lack of dust below some threshold radius that extends from a few AU to few tens of AU. This lack of dust is sometimes considered to track a lack of gas, but observational evidence for accretion onto the star in some cases shows that the cavities may be void of dust but not of gas. A narrow ring of hot dust is sometimes detected in the central AU of these discs (e.g., *Olofsson et al.*, 2012), and this structure is often claimed to be the signpost of a giant planet carving a big gap in the disc. It should be kept in mind, however, that the gap opened by a planet is usually much narrower than these observed depletions (see section 2.2.1), and rarely (completely) gas proof. There is here a missing ingredient between the numerical simulations of gas discs and observations. The outer edge of the gap opened by a giant planet corresponds to a pressure maximum. Dust decoupled from the gas tends to accumulate there, and does not drift through the gap. For typical disc densities and temperatures between 1 and 10 AU, decoupling is most efficient for dust particles of a few centimetres to a meter (e.g., *Ormel and Klahr*, 2010). Consequently, gaps appear wider in the dust component than in the gas component, and the inner disc could be void of dust even if not of gas (*Fouchet et al.*, 2010; *Zhu et al.*, 2012b). Note that these authors find that the smallest dust grains, which are well coupled to the gas, should have a distribution identical to that of the gas and be present inside the cavity. Therefore, the observation of a cavity should depend on the size of the tracked dust, that is

on the wavelength. Interpreting observations thus requires to decouple the dynamics of the gas and dust components. The coming years should see exciting, high resolution observations of protoplanetary discs, with for instance ALMA and MATISSE.

2.2.4. Formation of a circumplanetary disc

The formation of a circumplanetary disc accompanies the formation of a gap. The structure of a circumplanetary disc and the gas accretion rate onto the planet have been investigated through 2D hydrodynamical simulations (e.g., *Rivier et al.*, 2012), 3D hydrodynamical simulations (*D'Angelo et al.*, 2003; *Ayliffe and Bate*, 2009; *Machida et al.*, 2010; *Tanigawa et al.*, 2012), and more recently through 3D MHD simulations (*Uribe et al.*, 2013; *Gressel et al.*, 2013). *Gressel et al.* (2013) find accretion rates $\sim 0.01 M_\oplus$ yr^{-1}, in good agreement with previous 3D hydrodynamical calculations of viscous laminar discs. Also, in agreement with previous assessment in non-magnetic disc environments, they find that the accretion flow in the planet's Hill sphere is intrinsically three-dimensional, and that the flow of gas toward the planet moves mainly from high latitudes, rather than along the mid-plane of the circumplanetary disc.

Another issue is to address how a circumplanetary disc impacts migration. Being bound to the planet, the circumplanetary disc migrates at the same drift rate as the planet's. Issues arise in hydrodynamical simulations that discard the disc's self-gravity, as in this case the wave torque can only apply to the planet, and not to its circumplanetary material. This causes the circumplanetary disc to artificially slow down migration, akin to a ball and chain. This issue can be particularly important for type III migration (see Section 2.3). A simple workaround to this problem in simulations of non self-gravitating discs is to exclude the circumplanetary disc in the calculation of the torque exerted on the planet (see *Crida et al.*, 2009b). Another solution suggested by these authors and also adopted by *Pepliński et al.* (2008a) is to imprint to the circumplanetary disc the acceleration felt by the planet.

2.2.5. Evolution of the eccentricity and inclination of gap-opening planets

The early evolution of the Solar System in the primordial gas Solar nebula should have led the four giant planets to be in a compact resonant configuration, on quasi-circular and coplanar orbits (*Morbidelli et al.*, 2007; *Crida*, 2009). Their small but not zero eccentricities and relative inclinations are supposed to have been acquired after dispersal of the nebula, during a late global instability in which Jupiter and Saturn crossed their 2:1 mean motion resonance (*Tsiganis et al.*, 2005). This is the so-called Nice model.

Many massive exoplanets have much higher eccentricities than the planets in the Solar System. Also, recent measurements of the Rossiter-McLaughlin effect have reported several hot Jupiters with large obliquities, which indicates that massive planets could also acquire a large inclination

during their evolution.

Planet-disc interactions usually tend to damp the eccentricity and inclination of massive gap-opening planets (e.g., *Bitsch et al.*, 2013a; *Xiang-Gruess and Papaloizou*, 2013). Expressions for the damping timescales of eccentricity and inclination can be found in *Bitsch et al.* (2013a). In particular, this would indicate that type II migration should only produce hot Jupiters on circular and non-inclined orbits. There are, however, circumstances in which planets may acquire fairly large eccentricities and obliquities while embedded in their disk, which we summarise below.

Eccentricity– The 3:1 mean motion resonance between a planet and the disc excites eccentricity (*Lubow*, 1991). Thus, if a planet carves a gap that is wide enough for the eccentricity pumping effect of the 3:1 resonance to overcome the damping effect of all closer resonances, the planet eccentricity will grow (e.g., *Papaloizou et al.*, 2001, the disc eccentricity will grow as well). Hydrodynamical simulations show that planet-disc interactions can efficiently increase the eccentricity of planets over $\sim 5 - 10$ Jupiter masses (*Papaloizou et al.*, 2001; *Bitsch et al.*, 2013a; *Dunhill et al.*, 2013). Eccentricity values up to ≈ 0.25 have been obtained in *Papaloizou et al.* (2001).

Obliquity– Planets formed in a disk could have non-zero obliquities if the rotation axes of the star and the disc are not aligned. Several mechanisms causing misalignment have been proposed. One possibility is that the protoplanetary disc had material with differing angular momentum directions added to it at different stages of its life (e.g., *Bate et al.*, 2010). Alternatively, in dense stellar clusters, the interaction with a temporary stellar companion could tilt the disc's rotation axis (*Batygin*, 2012). However, both mechanisms should be extended by including the interaction between the disc and the magnetic field of the central star. This interaction might tilt the star's rotation axis, and lead to misalignments even in discs that are initially aligned with their star (*Lai et al.*, 2011).

2.3. Feedback of the coorbital dynamics on migration

Under most circumstances, such as those presented in the previous sections, the migration rate of a planet is provided by the value of the disc torque, which depends on the local properties of the underlying disc, but not on the migration rate itself. There are some circumstances, however, in which the torque also depends on the drift rate, in which case one has the constituting elements of a feedback loop, with potentially important implications for migration. This, in particular, is the case of giant or sub-giant planets embedded in massive discs, which deplete (at least partially) their horseshoe region.

2.3.1. Criterion for migration to run away

The corotation torque comes from material that executes horseshoe U-turns relative to the planet. Most of this material is trapped in the planet's horseshoe region. However, if there is a net drift of the planet with respect to the disc,

material outside the horseshoe region will execute a unique horseshoe U-turn relative to the planet, and by doing so will exchange angular momentum with the planet. This drift may come about because of migration, and/or because the disc has a radial viscous drift. The torque arising from orbit-crossing material naturally scales with the mass flow rate across the orbit, which depends on the relative drift of the planet and the disc. It thus depends on the migration rate.

For the sake of definiteness, we consider hereafter a planet moving inwards relative to the disc, but it should be kept in mind that the processes at work here are essentially reversible, so that they can also be applied to an outward moving planet. The picture above shows that the corotation torque on a planet migrating inwards has three contributions:

(i) The contribution of the inner disc material flowing across the orbit. As this material gains angular momentum, it exerts a negative torque on the planet which scales with the drift rate. It therefore tends to increase the migration rate, and yields a positive feedback on the migration.

(ii) The contribution of the coorbital material in the planet's horseshoe region. It is two-fold. A first component arises from the material that exerts a horseshoe drag on the planet, which corresponds to the same horseshoe drag as if there was no drift between the disc and the planet (see section 2.1.2).

(iii) Furthermore, as the material in the horseshoe region can be regarded as trapped in the vicinity of the planetary orbit, it has to move inward at the same rate as the planet. The planet then exerts on this material a negative torque, which scales with the drift rate. By the law of action-reaction, this trapped material yields a second, positive component of the horseshoe drag on the planet that scales with the drift rate. Thus, the contribution of the drifting trapped horseshoe material also yields a negative feedback on the migration.

If the surface density profile of the disc is unaltered by the planet, that is if the angular momentum profile of the disc is unaltered, then contributions (i) and (iii) exactly cancel out (*Masset and Papaloizou*, 2003). In that case, the net corotation torque reduces to contribution (ii), and the corotation torque expressions presented in section 2.1.2, which have been derived assuming that the planet is on fixed circular orbit, are valid regardless of the migration rate. Conversely, if the planet depletes, at least partly, its horseshoe region (when $\mathcal{P} \lesssim$ a few), contributions (i) and (iii) do not cancel out, and the net corotation torque depends on the migration rate.

The above description shows that the coorbital dynamics causes a feedback on migration when planets open a gap around their orbit. There are two key quantities to assess in order to determine when the feedback causes the migration to run away. The first quantity is called the coorbital mass deficit (δM). It represents the mass that should be added to the planet's horseshoe region so that it has the average surface density of the orbit-crossing flow. The second quantity is the sum of the planet mass (M_p) and of the circumplanetary disc mass (M_CPD), that is the quantity $\tilde{M}_\mathrm{p} = M_\mathrm{p} + M_\mathrm{CPD}$. As shown in *Masset and Papaloizou* (2003), two regimes may occur. If $\tilde{M}_\mathrm{p} > \delta M$, the coorbital dynamics accelerates the migration, but there is no runaway. On the contrary, if $\tilde{M}_\mathrm{p} < \delta M$, migration runs away. A more rigorous derivation performed by *Masset and Papaloizou* (2003) shows that the coorbital mass deficit actually features the inverse vortensity in place of the surface density, but the same qualitative picture holds.

2.3.2. Properties of type III migration

When migration runs away, the drift rate has an exponentially growing behaviour until the so-called fast regime is reached, in which the planet migrates a sizable fraction of the horseshoe width in less than a libration time. When that occurs, the drift rate settles to a finite, large value, which defines the regime of type III migration. As stressed earlier, this drift can either be outward or inward. The occurrence of type III migration with varying the planet mass, the disc's mass, aspect ratio, and viscosity was discussed in detail in *Masset* (2008). The typical migration timescale associated with type III migration, which depends on the disc mass (*Lin and Papaloizou*, 2010), is of the order of a few horseshoe libration times. For the large planetary masses prone to type III migration, which have wide horseshoe regions hence short libration times, this typically amounts to a few tens of orbits.

Type III migration can in principle be outwards. For this to happen, an initial seed of outward drift needs to be applied to the planet (*Pepliński et al.*, 2008b; *Masset and Papaloizou*, 2003; *Masset*, 2008). Nevertheless, all outward episodes of type III migration reported so far have been found to stall and revert back to inward migration. Interestingly, gravitationally unstable outer gap edges may provide a seed of outward type III migration and can bring massive planets to large orbital distances (*Lin and Papaloizou*, 2012; *Cloutier and Lin*, 2013). An alternative launching mechanism for outward type III migration is the outward migration of a resonantly locked pair of giant planets (*Masset and Snellgrove*, 2001, see also section 2.4.5), which is found to trigger outwards runaways at larger time (*Masset*, 2008).

The migration regime depends on how the coorbital mass deficit compares with the mass of the planet and its circumplanetary disc. It is thus important to describe correctly the build up of the circumplanetary material and the effects of this mass on the dynamics of the gas and planet. *D'Angelo et al.* (2005) find, using a nested grid code, that the mass reached by the CPD depends heavily on the resolution for an isothermal equation of state. *Pepliński et al.* (2008a) circumvent this problem by adopting an equation of state that not only depends on the distance to the star, but also on the distance to the planet, in order to prevent

an artificial flood of the CPD, and to obtain numerical convergence at high resolution. Furthermore, as we have seen in Section 2.2.4, in simulations that discard self-gravity, the torque exerted on the planet should exclude the circumplanetary disc. *D'Angelo et al.* (2005) find indeed that taking that torque into account may inhibit type III migration.

Type III migration has allowed to rule out a recent model of the Solar Nebula (*Desch*, 2007), more compact than the standard model of *Hayashi* (1981). Indeed, *Crida* (2009) has shown that Jupiter would be subject to type III migration in Desch's model and would not survive over the disc's lifetime. The occurrence of type III migration may thus provide an upper limit to the surface density of the disc models in systems known to harbor giant planets at sizable distances from their host stars.

It has been pointed out above that the exact expression of the coorbital mass deficit involves the inverse vortensity rather than the surface density across the horseshoe region. This has some importance in low-viscosity discs: vortensity can be regarded as materially conserved except during the passage through the shocks triggered by a giant planet, where vortensity is gained or destroyed. The corresponding vortensity perturbation can be evaluated analytically (*Lin and Papaloizou*, 2010). Eventually, the radial vortensity distribution around a giant planet exhibits a characteristic two-ring structure on the edges of the gap, which is unstable (*Lovelace et al.*, 1999; *Li et al.*, 2000) and prone to the formation of vortices (*Lin and Papaloizou*, 2010). The resulting vortensity profile determines the occurrence of type III migration. If vortices form at the gap edges, the planet can undergo non-smooth migration with episodes of type III migration that bring the planet inwards over a few Hill radii (a distance that is independent of the disc mass), followed by a stalling and a rebuild of the vortensity rings (*Lin and Papaloizou*, 2010).

The above results have been obtained for fixed-mass planets. However, for the high gas densities required by the type III migration regime, rapid growth may be expected. Using 3D hydrodynamical simulations with simple prescriptions for gas accretion, *D'Angelo and Lubow* (2008) find that a planetary core undergoing rapid runaway gas accretion does not experience type III migration, but goes instead from the type I to the type II migration regime. Future progress will be made using more realistic accretion rates, like those obtained with 3D radiation-hydrodynamics calculations (e.g., *D'Angelo and Bodenheimer*, 2013).

2.3.3. *Feedback of coorbital dynamics on type I migration*

It has been shown that type I migration in adiabatic discs could feature a kind of feedback reminiscent of type III migration. The reason is that in adiabatic discs, the corotation torque depends on the position of the stagnation point relative to the planet (see section 2.1.2). This position, in turn, depends on the migration rate, so that there is here as well a feedback of the coorbital dynamics on migration. *Masset and Casoli* (2009) found that this feedback on type I migra-
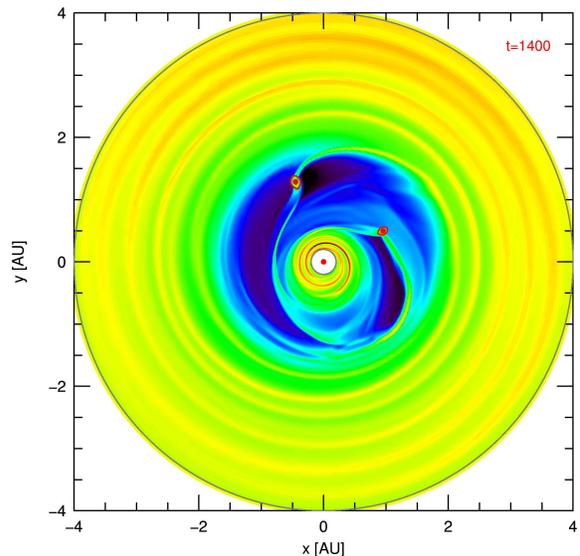

Fig. 4.— Surface density of a disc with two Jupiter-mass planets located in a common gap, and engaged in a 2:1 mean-motion resonance. The inner planet mainly interacts with the inner disc, and the outer planet with the outer disc, which helps to maintain the resonant configuration. From *Kley and Nelson* (2012).

tion is negative, and that is has only a marginal impact on the drift rate for typical disc masses.

2.4. Orbital evolution of multi-planet systems

So far, we have examined the orbital evolution of a single planet in a protoplanetary disc, while about $1/3$ of confirmed exoplanets reside in multi-planetary systems (see exoplanets.org). In such systems, the gravitational interaction between planets can significantly influence the planet orbits, leading, in particular, to important resonant processes which we describe below. A fair number of multi-planetary systems is known to have at least two planets in mean-motion resonance. *Szuszkiewicz and Podlewska-Gaca* (2012) list for example 32 resonant or near-resonant systems, with many additional Kepler candidate systems. The mere existence of these resonant systems is strong evidence that dissipative mechanisms changing planet semi-major axes must have operated. The probability of forming resonant configurations in situ is likely small (e.g., *Beaugé et al.*, 2012).

2.4.1. *Capture in mean-motion resonance*

We consider a system of two planets that undergo migration in their disc. If the migration drift rates are such that the mutual separation between the planets increases, i.e. when divergent migration occurs, the effects of planet-planet interactions are small and no resonant capture occurs. Conversely, resonant capture occurs for convergent migration under quite general conditions, which we discuss below.

Planets can approach each other from widely separated orbits if they have fairly different migration rates, or if

they form in close proximity and are sufficiently massive to carve a common gap (see Fig. 4). In the latter case, the outer disc pushes the outer planet inwards, the inner disc pushes the inner planet outwards, causing convergence. If the planets approach a commensurability, where the orbital periods are the ratio of two integers, orbital eccentricities will be excited and resonant capture may occur. Whether or not resonant capture occurs hinges primarily on the time the planets take to cross the resonance. Capture requires the convergent migration timescale to be longer than the libration timescale associated with the resonance width (*Snellgrove et al.*, 2001). Otherwise, the two-planet system does not have enough time for the resonance to be excited: the two planets will pass through the resonance and no capture will occur (e.g., *Quillen*, 2006; *Mustill and Wyatt*, 2011). Due to the sensitivity of the resonant capture to the migration process, the interpretation of observed resonant planetary systems provides important clues about the efficiency of disc-planets interactions.

A mean-motion resonance between two planets occurs when their orbital frequencies satisfy

$$(p + q)\Omega_2 - p\Omega_1 = 0, \tag{12}$$

where Ω_i is the angular velocity of the two planets, and where subscripts 1 and 2 refer to quantities of the inner and outer planets, respectively. In Eq. (12), q and p are positive integers, and q denotes the order of the resonance. The above condition for a mean-motion resonance can be recast in terms of the planets semi-major axes, a_i, as

$$\frac{a_2}{a_1} = \left(\frac{p + q}{p}\right)^{2/3}. \tag{13}$$

Formally, a system is said to be in a $p + q : p$ mean-motion resonance if at least one of the resonant angles is librating, i.e. has a dynamical range smaller than 2π. The resonant angles ($\phi_{1,2}$) are defined as

$$\phi_{1,2} = (p + q)\lambda_2 - p\lambda_1 - q\,\varpi_{1,2}, \tag{14}$$

where λ_i denotes the planets longitude, and ϖ_i the longitude of their pericentre. The difference in pericentre longitudes is often used to characterise resonant behaviour. For instance, when that quantity librates, the system is said to be in apsidal corotation. This means that the two apsidal lines of the resonant planets are always nearly aligned, or maintain a constant angle between them. This is the configuration that the planets end up with when they continue their inward migration after capture in resonance (e.g., *Kley et al.*, 2004).

Several bodies in our Solar System are in mean-motion resonance. For example, the Jovian satellites Io, Europa and Ganymede are engaged in a so-called 1:2:4 Laplace resonance, while Neptune and Pluto (as well as the Plutinos) are in a 3:2 mean-motion resonance. However, out of the 8 planets in the Solar System, not a single pair is presently in a mean-motion resonance. According to the Nice model for

the early Solar System, this might have been different in the past (see section 2.2.5).

The question of which resonance the system may end up in depends on the mass, the relative migration speed, and the initial separation of the planets (*Nelson and Papaloizou*, 2002). Because the 2:1 resonance ($p = 1, q = 1$) is the first first-order resonance that two initially well-separated planets encounter during convergent migration, it is common for planets to become locked in that resonance, provided convergent migration is not too rapid.

After a resonant capture, the eccentricities increase and the planets generally migrate as a joint pair, maintaining a constant orbital period ratio (see, however, the last two paragraphs in section 3.1.2). Continued migration in resonance drives the eccentricities up, and they would increase to very large values in the absence of damping agents, possibly rendering the system unstable. The eccentricity damping rate by the disc, $\dot{e}$, is often parametrized in terms of the migration rate $\dot{a}$ as

$$\left|\frac{\dot{e}}{e}\right| = K\left|\frac{\dot{a}}{a}\right|, \tag{15}$$

with K a dimensionless constant. For low-mass planets, typically below 10 to 20 $M_\oplus$, eccentricity damping occurs much more rapidly than migration: $K \sim \mathcal{O}[h^{-2}] \sim$ a few hundred in locally isothermal discs (see Section 2.1.5) and may take even larger values in radiative discs. High-mass planets create gaps in their disc (see Section 2.2) and the eccentricity damping is then strongly reduced. For the massive planets in the GJ 876 planetary system, the three-body integrations of *Lee and Peale* (2002), in which migration is applied to the outer planet only, showed that $K \sim 100$ can reproduce the observed eccentricities. If massive planets orbit in a common gap, as in Fig. 4, the disc parts on each side of the gap may act as damping agents, and it was shown by the 2D hydrodynamical simulations of *Kley et al.* (2004) that such configuration gives $K \sim 5$–10.

Disc turbulence adds a stochastic component to convergent migration, which may prevent resonant capture or maintenance of a resonant configuration. This has been examined in N-body simulations with prescribed models of disc-planet interactions and of disc turbulence (e.g., *Ketchum et al.*, 2011; *Rein*, 2012a), and in hydrodynamical simulations of planet-disc interactions with simplified turbulence models (*Pierens et al.*, 2011; *Paardekooper et al.*, 2013).

2.4.2. *Application to specific multi-planet systems*

Application of above considerations leads to excellent agreement between theoretical evolution models of resonant capture and the best observed systems, in particular GJ 876 (*Lee and Peale*, 2002; *Kley et al.*, 2005; *Crida et al.*, 2008). Because resonant systems most probably echo an early formation via disc-planets interactions, the present dynamical properties of observed systems can give an indicator of evolutionary history. This has been noticed recently in the system HD 45364, where two planets in 3:2

resonance have been discovered by *Correia et al.* (2009). Fits to the data give semi-major axes $a_1 = 0.681\mathrm{AU}$ and $a_2 = 0.897\mathrm{AU}$, and eccentricities $e_1 = 0.168$ and $e_2 = 0.097$, respectively. Non-linear hydrodynamic simulations of disc-planets interactions have been carried out for this system by *Rein et al.* (2010). For suitable disc parameters, the planets enter the 3:2 mean-motion resonance through convergent migration. After the planets reached their observed semi-major axis, a theoretical RV-curve was calculated. Surprisingly, even though the simulated eccentricities ($e_1 = 0.036, e_2 = 0.017$) differ significantly from the data fits, the theoretical model fits the observed data points as well as the published best fit solution (*Rein et al.*, 2010). The pronounced dynamical differences between the two orbital fits, which both match the existing data, can only be resolved with more observations. Hence, HD 45364 serves as an excellent example of a system in which a greater quantity and quality of data will constrain theoretical models of this interacting multi-planetary system.

2.4.3. Eccentricity and inclination excitations

Another interesting observational aspect where convergent migration due to disc-planets interactions may have played a prominent role is the high mean eccentricity of extrasolar planets (~ 0.3). As discussed above, for single planets, disc-planet interactions nearly always lead to eccentricity damping, or, at best, to modest growth for planets of few Jupiter masses (see section 2.2.5). Strong eccentricity excitation may occur, however, during convergent migration and resonant capture of two planets. Convergent migration of three massive planets in a disc may lead to close encounters that significantly enhance planet eccentricities (*Marzari et al.*, 2010) and inclinations. In the latter case, an inclination at least $\gtrsim 20 - 40$ degrees between the planetary orbit and the disc may drive Kozai cycles. Under disc-driven Kozai cycles, the eccentricity increases to large values and undergoes damped oscillations with time in antiphase with the inclination (*Teyssandier et al.*, 2013; *Bitsch et al.*, 2013a; *Xiang-Gruess and Papaloizou*, 2013).

As the disc slowly dissipates, damping will be strongly reduced. This may leave a resonant system in an unstable configuration, triggering dynamical instabilities (*Adams and Laughlin*, 2003). Planet-planet scattering may then pump eccentricities to much higher values. This scenario has been proposed to explain the observed broad distribution of exoplanet eccentricities (*Chatterjee et al.*, 2008; *Jurić and Tremaine*, 2008; *Matsumura et al.*, 2010). However, note that the initial conditions taken in these studies are unlikely to result from the evolution of planets in a protoplanetary disc (*Lega et al.*, 2013).

Using N-body simulations with 2 or 3 giant planets and prescribed convergent migration, but no damping, *Libert and Tsiganis* (2009, 2011) found that, as the eccentricities raise to about 0.4 due to resonant interactions, planet inclinations could also be pumped under some conditions. The

robustness of this mechanism needs to be checked by including eccentricity and inclination damping by the disc.

2.4.4. Low-mass planets

Disc-planets interactions of several protoplanets ($5 - 20 M_{\oplus}$) undergoing type I migration leads to crowded systems (*Cresswell and Nelson*, 2008). These authors find that protoplanets often form resonant groups with first-order mean-motion resonances having commensurabilities between 3:2 - 8:7 (see also *McNeil et al.*, 2005; *Papaloizou and Szuszkiewicz*, 2005). Strong eccentricity damping allows these systems to remain stable during their migration. In general terms, these simulated systems are reminiscent of the low-mass planet systems discovered by the Kepler mission, like Kepler-11 (*Lissauer et al.*, 2011a). The proximity of the planets to the star in that system, and their near coplanarity, hints strongly toward a scenario of planet formation and migration in a gaseous protoplanetary disc.

2.4.5. Possible reversal of the migration

Masset and Snellgrove (2001) have shown that a pair of close giant planets can migrate outwards. In this scenario, the inner planet is massive enough to open a deep gap around its orbit and undergoes type II migration. The outer, less massive planet opens a partial gap and migrates inwards faster than the inner planet. If convergent migration is rapid enough for the planets to cross the 2:1 mean-motion resonance, and to lock in the 3:2 resonance, the planets will merge their gap and start migrating outwards together. The inner planet being more massive than the outer one, the (positive) torque exerted by the inner disc is larger than the (negative) torque exerted by the outer disc, which results in the planet pair moving outwards. Note that to maintain joint outward migration on the long term, gas in the outer disc has to be funnelled to the inner disc upon embarking onto horseshoe trajectories relative to the planet pair. Otherwise, gas would pile up at the outer edge of the common gap, much like a snow-plough, and the torque balance as well as the direction of migration would ultimately reverse.

The above mechanism of joint outward migration of a resonant planet pair relies on an asymmetric density profile across the common gap around the two planets. This mechanism is therefore sensitive to the disc's aspect ratio, viscosity, and to the mass ratio between the two planets, since they all impact the density profile within and near the common gap. If, for instance, the outer planet is too small, the disc density beyond the inner planet's orbit will be too large to reverse the migration of the inner planet (and, thus, of the planet pair). Conversely, if the outer planet is too big, the torque imbalance on each side of the common gap will favour joint inward migration. Numerical simulations by (*D'Angelo and Marzari*, 2012) showed that joint outward migration works best when the mass ratio between the inner and outer planets is comparable to that of Jupiter and Saturn (see also *Pierens and Nelson*, 2008). In particular, *Morbidelli and Crida* (2007) found that the Jupiter-Saturn

pair could avoid inward migration and stay beyond the ice line during the gas disc phase. Their migration rate depends on the disc properties, but could be close to stationary for standard values.

More recently, *Walsh et al.* (2011) have proposed that Jupiter first migrated inwards in the primordial Solar nebula down to ~ 1.5 AU, where Saturn caught it up. Near that location, after Jupiter and Saturn have merged their gap and locked into the 3:2 mean-motion resonance, both planets would have initiated joint outward migration until the primordial nebula dispersed. This scenario is known as *the Grand Tack*, and seems to explain the small mass of Mars and the distribution of the main asteroid belt.

3. PLANET FORMATION AND MIGRATION: COMPARISON WITH OBSERVATIONS

The previous section has reviewed basics of, and recent progress on planet-disc interactions. We continue in this section with a discussion on the role played by planet-disc interactions in the properties and architecture of observed planetary systems. Section 3.1 starts with planets on short-period orbits. Emphasis is put on hot Jupiters, including those with large spin-orbit misalignments (section 3.1.1), and on the many low-mass candidate systems uncovered by the Kepler mission (section 3.1.2). Section 3.2 then examines how planet-disc interactions could account for the massive planets recently observed at large orbital separations by direct imaging techniques. Finally, section 3.3 addresses how well global models of planet formation and migration can reproduce the statistical properties of exoplanets.

3.1. Planets on short-period orbits

3.1.1. Giant planets

The discovery of 51 Pegasi b (*Marcy and Butler*, 1995) on a close-in orbit of 4.2 days as the first example of a hot Jupiter led to the general view that giant planets, which are believed to have formed beyond the ice line at $\gtrsim 1$ AU, must have migrated inwards to their present locations. Possible mechanisms for this include type II migration (see section 2.2) and either planet-planet scattering, or Kozai oscillations induced by a distant companion leading to a highly eccentric orbit which is then circularized as a result of tidal interaction with the central star (see, e.g., *Papaloizou and Terquem*, 2006; *Kley and Nelson*, 2012; *Baruteau and Masset*, 2013, and references therein). The relative importance of these mechanisms is a matter of continuing debate.

The relationship between planet mass and orbital period for confirmed exoplanets on short-period orbits is shown in Fig. 5. The hot Jupiters are seen to be clustered in circular orbits at periods in the range $3 - 5$ days. For planet masses in the range $0.01 - 0.1$ Jupiter masses, there is no corresponding clustering of orbital periods, indicating that this is indeed a feature associated with hot Jupiters.

Measurements of the Rossiter-McLaughlin effect (e.g., *Triaud et al.*, 2010) indicate that around one third of hot
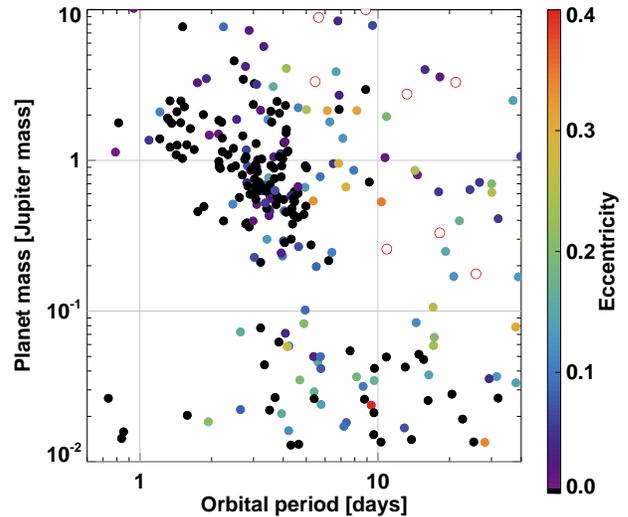

Fig. 5.— Mass as a function of orbital period for confirmed exoplanets on short-period orbits. The colour of the dots represents the magnitude of the orbital eccentricity as indicated in the colour bar (white dots with a red circle correspond to eccentricities larger than 0.4). Data were extracted from exoplanets.org.

Jupiters orbit in planes that are significantly misaligned with the equatorial plane of the central star. This is not expected from disc-planet interactions leading to type II migration, and so has led to the alternative mechanisms being favoured. Thus *Albrecht et al.* (2012) propose that hot Jupiters are placed in an isotropic distribution through dynamical interactions, and are then circularized by tides, with disc-driven migration playing a negligible role. They account for the large fraction of misaligned hot Jupiters around stars with effective temperatures $\gtrsim 6200$ K, and the large fraction of aligned hot Jupiters around cooler stars, as being due to a very large increase in the effectiveness of the tidal processes causing alignment for the cooler stars.

However, there are a number of indications that the process of hot Jupiter formation does not work in this way, and that a more gentle process such as disc-driven migration has operated on the distribution. We begin by remarking the presence of significant eccentricities for periods $\gtrsim 6$ days in Fig. 5. The period range over which tidal effects can circularize the orbits is thus very limited. Giant planets on circular orbits with periods greater than 10 days, which are interior to the ice line, must have been placed there by a different mechanism. For example, 55 Cnc b, a 0.8 M_J planet on a 14 day, near-circular orbit exterior to hot super-Earth 55 Cnc e (*Dawson and Fabrycky*, 2010) is a good case for type II migration having operated on that system. There is no reason to suppose that a smooth delivery of hot Jupiters through type II migration would not function at shorter periods.

There are also issues with the effectiveness of the tidal process (see *Rogers and Lin*, 2013). It has to align inclined circular orbits without producing inspiral into the central star. To avoid the latter, the components of the tidal po-

tential that act with non-zero forcing frequency in an iner-
tial frame when the star does not rotate, have to be inef-
fective. Instead one has to rely on components that appear
to be stationary in this limit. These have a frequency that
is a multiple of the stellar rotation frequency, expected to
be significantly less than the orbital frequency, as viewed
from the star when it rotates. As such components depend
only on the time averaged orbit, they are insensitive to the
sense of rotation in the orbit. Accordingly there is a sym-
metry between prograde and retrograde aligning orbits with
respect to the stellar equatorial plane. This is a strict sym-
metry when the angular momentum content of the star is
negligible compared to that of the orbit, otherwise there is
a small asymmetry (see *Rogers and Lin*, 2013). Notably,
a significant population of retrograde orbits with aligned
orbital planes, that is expected in this scenario, is not ob-
served.

   Dawson and Murray-Clay (2013) have recently exam-
ined the dependence of the relationship between mass and
orbital period on the metallicity of the central star. They
find that the pile up for orbital periods in the range $3 - 5$
days characteristic of hot Jupiters is only seen at high metal-
licity. In addition, high eccentricities, possibly indicative of
dynamical interactions, are also predominantly seen at high
metallicity. This indicates multi-planet systems in which
dynamical interactions leading to close orbiters occur at
high metallicity, and that disc-driven migration is favoured
at low metallicity.

   Finally, misalignments between stellar equators and or-
bital planes may not require strong dynamical interactions.
Several mechanisms may produce misalignments between
the protoplanetary disc and the equatorial plane of its host
star (see section 2.2.5). Another possibility is that internal
processes within the star, such as the propagation of gravity
waves in hot stars, lead to different directions of the angular
momentum vector in the central and surface regions (e.g.,
Rogers et al., 2012).

3.1.2. Low-mass planets

The Kepler mission has discovered tightly packed plane-
tary systems orbiting close to their star. Several have been
determined to be accurately coplanar, which is a signature
of having formed in a gaseous disc. These include KOI
94 and KOI 25 (*Albrecht et al.*, 2013), KOI 30 (*Sanchis-
Ojeda et al.*, 2012), and Kepler 50 and Kepler 55 (*Chaplin
et al.*, 2013). We remark that if one supposed that formation
through in situ gas free accumulation had taken place, for
planets of a fixed type, the formation time scale would be
proportional to the product of the local orbital period and
the reciprocal of the surface density of the material mak-
ing up the planets (e.g., *Papaloizou and Terquem*, 2006).
For a fixed mass this is proportional to $r^{3.5}$. Scaling from
the inner Solar system, where this time scale is taken to
be $\sim 3 \times 10^8$ yr (*Chambers and Wetherill*, 1998), it be-
comes $\lesssim 10^5$ yr for $r < 0.1$ AU. Note that this time scale is
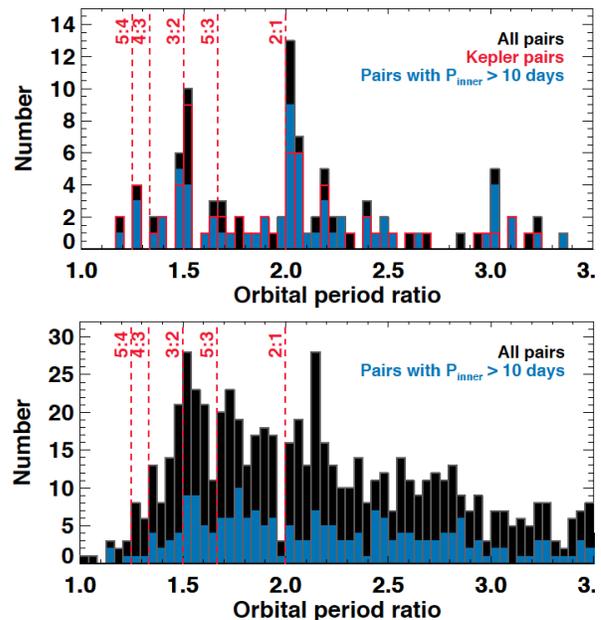even shorter for more massive and more compact systems.

Fig. 6.— The period ratio histogram for confirmed exoplanets
is shown in the upper panel. The same histogram is shown in the
lower panel for Kepler candidates from Quarters 1 to 8. Vertical
dashed lines show the period ratio of a few mean-motion reso-
nances. Data were extracted from exoplanets.org.

This points to a possible formation during the disc lifetime,
although the formation process should be slower and qui-
eter in a disc, as protoplanets are constrained to be in non-
overlapping near circular orbits. Under this circumstance,
disc-planet interactions cannot be ignored.

   Notably, *Lissauer et al.* (2011b) found that a signifi-
cant number of Kepler multiplanet candidate systems con-
tain pairs that are close to first-order resonances. They
also found a few multi-resonant configurations. An exam-
ple is the four planet system KOI-730 which exhibits the
mean motion ratios 8:6:4:3. More recently, *Steffen et al.*
(2013) confirmed the Kepler 60 system which has three
planets with the inner pair in a 5:4 commensurability and
the outer pair in a 4:3 commensurability. However, most of
the tightly packed candidate systems are non-resonant.

   The period ratio histogram for all pairs of confirmed ex-
oplanet systems is shown in the upper panel of Fig. 6.
This shows prominent spikes near the main first-order res-
onances. However, this trend is biased because many of
the Kepler systems were validated through observing tran-
sit timing variations, which are prominent for systems near
resonances. The lower panel of this figure shows the same
histogram for Kepler candidate systems announced at the
time of writing (Quarters 1-8). In this case, although there
is some clustering in the neighbourhood of the 3:2 commen-
surability and an absence of systems at exact 2:1 commen-
surability, with there being an overall tendency for systems
to have period ratios slightly larger than exact resonant val-
ues, there are many non resonant systems.

   At first sight, this appears to be inconsistent with results

from the simplest theories of disc-planet interactions, for which convergent migration is predicted to form either resonant pairs (*Papaloizou and Szuszkiewicz*, 2005) or resonant chains (*Cresswell and Nelson*, 2006). However, there are features not envisaged in that modelling which could modify these results, which we briefly discuss below. These fall into two categories: (i) those operating while the disc is still present, and (ii) those operating after the disc has dispersed. An example of the latter type is the operation of tidal interactions with the central star, which can cause two planet systems to increase their period ratios away from resonant values (*Papaloizou*, 2011; *Lithwick and Wu*, 2012; *Batygin and Morbidelli*, 2013). However, this cannot be the only process operating as Fig. 6 shows that the same period ratio structure is obtained for periods both less than and greater than 10 days. We also note that compact systems with a large number of planets can be close to dynamical instability through the operation of Arnold' diffusion (see, e.g., the analysis of Kepler 11 by *Migaszewski et al.*, 2012). Thus it is possible that memory of the early history of multi-planet systems is absent from their current configurations.

When the disc is present, stochastic forcing due to the presence of turbulence could ultimately cause systems to diffuse out of resonance (e.g., *Pierens et al.*, 2011; *Rein*, 2012a). When this operates, resonances may be broken and period ratios may both increase and decrease away from resonant values. *Paardekooper et al.* (2013) employed stochastic fluctuations in order to enable lower order resonances to be diffused through under slow convergent migration. In this way, they could form a 7:6 commensurability in their modelling of the Kepler 36 system.

Another mechanism that could potentially prevent the formation of resonances in a disc involves the influence of each planet's wakes on other planets. The dissipation induced by the wake of a planet in the coorbital region of another planet causes the latter to be effectively repelled. This repulsion might either prevent the formation of resonances, or result in an increase in the period ratio from a resonant value. *Podlewska-Gaca et al.* (2012) considered a $5.5M_\oplus$ super-Earth migrating in a disc towards a giant planet. The upper panel in Fig. 7 shows the time evolution of the super-Earth's semi-major axis when orbiting exterior to a planet of one Jupiter or two Jupiter masses. We see that the super-Earth's semi-major axis attains a minimum and ultimately increases. Thus a resonance is not maintained. The lower panel shows the disc's surface density at one illustrative time: the super-Earth (grey arrow) feels a head wind from the outer wake of the hot Jupiter, which leads to the super Earth being progressively repelled. This mechanism could account for the observed scarcity of super-Earths on near-resonant orbits exterior to hot Jupiters.

A similar effect was found in disc-planets simulations with two partial gap-opening planets by *Baruteau and Papaloizou* (2013). This is illustrated in Fig. 8. The orbital period ratio between the planets initially decreases until the planets get locked in the 3:2 mean-motion resonance. The period ratio then increases away from the resonant ratio as
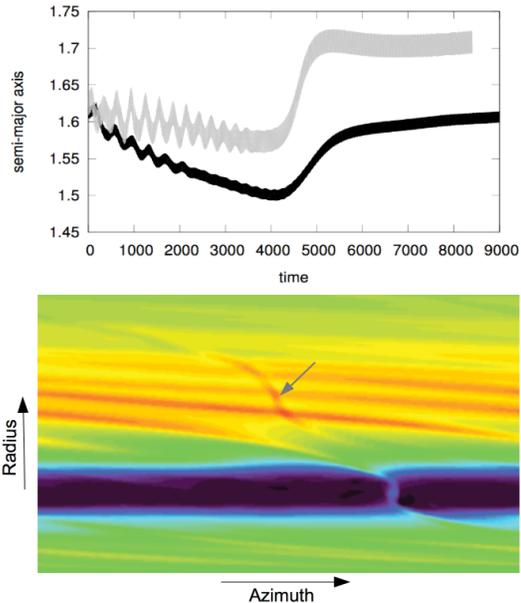

Fig. 7.— Top: semi-major axis evolution of a $5.5M_\oplus$ super-Earth orbiting exterior to an inwardly migrating giant planet of 1 M_J (dark line) or 2 M_J (light grey line) that is initially located at $a = 1$. Time shown in x-axis is 2π times the initial orbital period of the giant planet. Bottom: disc's surface density for the one Jupiter mass case. The super-Earth's location is spotted by a grey arrow. Adapted from *Podlewska-Gaca et al.* (2012).

a result of wake-planet interactions. The inset panel shows a density contour plot where the interaction of the planets with each other's wakes is clearly seen. Divergent evolution of a planet pair through wake-planet interactions requires some non-linearity, and so will not work with pure type I migration ($\mathcal{P} \gg 1$), but not so much that the gaps become totally cleared (*Baruteau and Papaloizou*, 2013). This mechanism works best for partial gap-opening planets ($\mathcal{P} \sim$ a few, $q \sim h^3$), which concern super-Earth to Neptune mass planets in discs with aspect ratio $h \lesssim 3\%$ (expected in inner disc regions), or Saturn-mass planets if $h \sim 5\%$. These results show circumstances where convergent migration followed by attainment of stable strict commensurability may not be an automatic consequence of disc-planet interactions. Wake-planet interactions could explain why near-resonant planet pairs amongst Kepler's multiple candidate systems tend to have period ratios slightly greater than resonant.

3.2. Planets on long-period orbits

In the past decade, spectacular progress in direct imaging techniques have uncovered more than 20 giant planets with orbital separations ranging from about ten to few hundred AU. The four planets in the HR 8799 system (*Marois et al.*, 2010) or β−Pictoris b (*Lagrange et al.*, 2010) are remarkable examples. The discoveries of these *cold Jupiters* have challenged theories of planet formation and evolution. We review below the mechanisms that have been proposed to
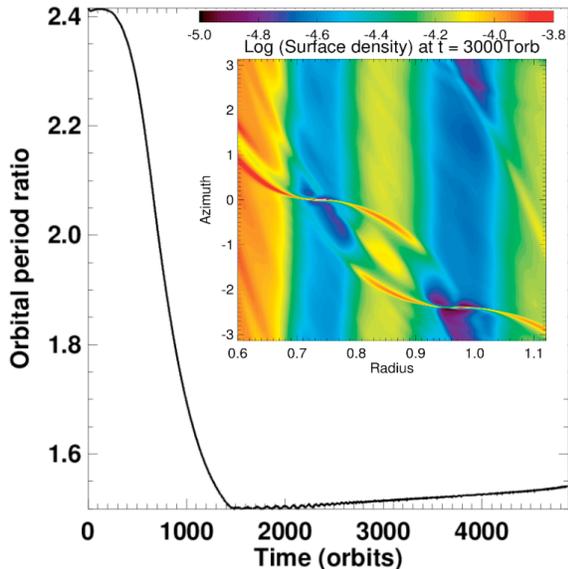
Fig. 8.— Evolution of the orbital period ratio between an $13M_\oplus$ outer planet and an $15M_\oplus$ inner planet. The period ratio increases from the 3:2 resonant ratio due to wake-planet interactions. These interactions are visible in the disc's surface density shown in the inset image. Adapted from *Baruteau and Papaloizou* (2013).

account for the cold Jupiters.

3.2.1. Outward migration of planets formed further in?

In the core-accretion scenario for planet formation, it is difficult to form Jupiter-like planets in isolation beyond ~ 10 AU from a Sun-like star (*Pollack et al.*, 1996; *Ida and Lin*, 2004, and see the chapter by Helled et al.). Could forming Jupiters move out to large orbital separations in their disc? Outward type I migration followed by rapid gas accretion is possible, but the maximum orbital separation attainable through type I migration is uncertain (see sections 2.1.2 and 2.1.4). Planets in the Jupiter-mass range are expected to open an annular gap around their orbit (see section 2.2.1). If a deep gap is carved, inward type II migration is expected. If a partial gap is opened, outward type III migration could occur under some circumstances (see section 2.3), but numerical simulations have shown that it is difficult to sustain this type of outward migration over long timescales (*Masset and Papaloizou*, 2003; *Pepliński et al.*, 2008b). It is therefore unlikely that a *single* massive planet formed through the core-accretion scenario could migrate to several tens or hundreds of AU.

It is possible, however, that a pair of close giant planets may migrate outwards according to the mechanism described in Section 2.4.5. For non-accreting planets, this mechanism could deliver two near-resonant giant planets at orbital separations comparable to those of the cold Jupiters (*Crida et al.*, 2009a). However, this mechanism relies on the outer planet to be somewhat less massive than the inner one. Joint outward migration may stall and eventually reverse if the outer planet grows faster than the inner one

(*D'Angelo and Marzari*, 2012). Numerical simulations by these authors showed that it is difficult to reach orbital separations typical of the cold Jupiters.

3.2.2. Planets scattered outwards?

The fraction of confirmed planets known in multi-planetary systems is about $1/3$ (see, e.g., exoplanets.org), from which nearly $2/3$ have an estimated minimum mass (the remaining $1/3$ comprises Kepler multiple planets confirmed by TTV, and for which an upper mass estimate has been obtained based on dynamical stability; see for example *Steffen et al.* (2013)). More than half of the confirmed multiple planets having a lower mass estimate are more massive than Saturn, which indicates that the formation of several giant planets in a protoplanetary disc should be quite common. Smooth convergent migration of two giant planets in their parent disc should lead to resonant capture followed by joint migration of the planet pair (e.g., *Kley et al.*, 2004). Dispersal of the gas disc may trigger the onset of dynamical instability, with close encounters causing one of the two planets to be scattered to large orbital separations (*Chatterjee et al.*, 2008). A system of three giant planets is more prone to dynamical instability, and disc-driven convergent migration of three giant planets may induce planet scattering even in quite massive protoplanetary discs (*Marzari et al.*, 2010; *Moeckel and Armitage*, 2012). Planet scattering before or after disc dispersal could thus be a relevant channel for delivering one or several massive planets to orbital separations comparable to the cold Jupiters'. It could also account for the observed free-floating planets.

3.2.3. Formation and evolution of planets by gravitational instability?

Giant planets could also form after the fragmentation of massive protoplanetary discs into clumps through the gravitational instability (GI). The GI is triggered as the well-known Toomre-Q parameter is ~ 1 and the disc's cooling timescale approaches the dynamical timescale (*Gammie*, 2001; *Rafikov*, 2005). The later criterion is prone to some uncertainty due to the stochastic nature of fragmentation (*Paardekooper*, 2012). The GI could trigger planet formation typically beyond 30 AU from a Sun-like star.

How do planets evolve once fragmentation is initiated? First, GI-formed planets are unlikely to stay in place in their gravito-turbulent disc. Since these massive planets form in about a dynamical timescale, they rapidly migrate to the inner parts of their disc, having initially no time to carve a gap around their orbit (*Baruteau et al.*, 2011b; *Zhu et al.*, 2012a; *Vorobyov*, 2013, see Fig. 9). These inner regions should be too hot to be gravitationally unstable, and other sources of turbulence, like the MRI, will set the background disc profiles and the level of turbulence. The rapid inward migration of GI-formed planets could then slow down or even stall, possibly accompanied by the formation of a gap around the planet's orbit. Gap-opening may also occur if significant gas accretion occurs during the initial stage of
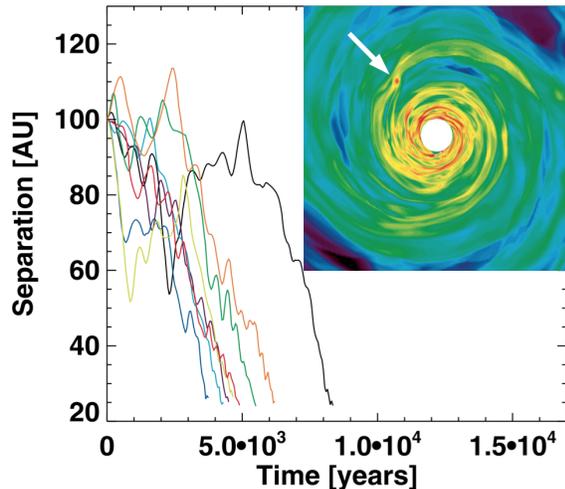
Fig. 9.— Semi-major axis evolution of a Jupiter-mass planet formed in a self-gravitating turbulent disc at 100 AU from a Solar-mass star. Different curves are for different simulations with varying initial conditions. The inset image shows the disc's surface density in one of these simulations, and the arrow spots the planet's location. Adapted from *Baruteau et al.* (2011b).

rapid migration (*Zhu et al.*, 2012a), which may promote the survival of inwardly migrating clumps. Planet–planet interactions, which may result in scattering events, mergers, or resonant captures in a disc, should also play a prominent role in shaping planetary systems formed by GI. The near resonant architecture of the HR 8799 planet system could point to resonant captures after convergent migration in a gravito-turbulent disc.

Furthermore, gas clumps progressively contract as they cool down. As clumps initially migrate inwards, they may experience some tidal disruption, a process known as tidal downsizing. This process could deliver a variety of planet masses in the inner parts of protoplanetary discs (*Boley et al.*, 2010; *Nayakshin*, 2010).

3.3. Planet formation with migration: population synthesis and N-body simulations

All of the disc-driven migration scenarios discussed in this review have some dependence on the planet mass, so it is necessary to consider the combined effects of mass growth and migration when assessing the influence of migration on the formation of planetary systems. Two approaches that have been used extensively for this purpose are planetary population synthesis and N-body simulations, both of which incorporate prescriptions for migration.

Population synthesis studies use Monte-Carlo techniques to construct synthetic planetary populations, with the aim of determining which combinations of model ingredients lead to statistically good fits to the observational data (orbital elements and masses in particular, but in more recent developments planetary radii and luminosities are also calculated as observables; see, e.g., *Mordasini et al.*, 2012). In principle this allows the mass-period and mass-radius

relation for gaseous exoplanets to be computed. Input variables that form the basis of the Monte-Carlo approach include initial gas disc masses, gas-to-dust ratios, and disc photoevaporation rates, constrained by observational data. The advantages of population synthesis studies lie in their computational speed and ability to include a broad range of physical processes. This allows the models to treat elements of the physics (such as gas envelope accretion, or ablation of planetesimals as they pass through the planet envelope, for example) much more accurately than is possible in N-body simulations. A single realisation of a Monte-Carlo simulation consists of drawing a disc model from the pre-defined distribution of possibilities and introducing a single low-mass planetary embryo in the disc at a random location within a predefined interval in radius. Accretion of planetesimals then proceeds, followed by gas envelope settling as the core mass grows. Runaway gas accretion to form a gas giant may occur if the core mass reaches the critical value. Further implementation details are provided in the chapter on planetary population synthesis by Benz et al. in this volume.

The main advantages of the N-body approach are that they automatically include an accurate treatment of planet-planet interactions that is normally missing from the 'single-planet-in-a-disc' Monte-Carlo models, they capture the competitive accretion that is inherently present in the oligarchic picture of early planet formation, and they incorporate giant impacts between embryos that are believed to provide the crucial last step in terrestrial planet formation. At present, however, gas accretion has been ignored or treated in a crude manner in N-body models. As such, population synthesis models can provide an accurate description of the formation of a gas giant planet, whereas N-body models are well-suited to examining the formation of systems of lower mass terrestrial, super-Earth and core-dominated Neptune-like bodies.

As indicated above, the basis of almost all published population synthesis models has been the core-accretion scenario of planetary formation, combined with simple prescriptions for type I and type II migration and viscous disc evolution (*Armitage et al.*, 2002; *Ida and Lin*, 2004; *Alibert et al.*, 2005; *Mordasini et al.*, 2009a). A notable exception is the recent population synthesis study based on the disc fragmentation model (*Forgan and Rice*, 2013). Almost all studies up to the present time have adopted type I migration rates similar to those arising from Eq. (1), supplemented with an arbitrary reduction factor that slows the migration. The influence of the vortensity and entropy-related horseshoe drag discussed in Sect. 2.1.2 has not yet been explored in detail, although a couple of recent preliminary explorations that we describe below have appeared in the literature.

Ida and Lin (2008), *Mordasini et al.* (2009a) and *Mordasini et al.* (2009b) consider the effects of type I and type II migration in their population synthesis models. Although differences exist in the modelling procedures, these studies all conclude that unattenuated type I migration leads to

planet populations that do not match the observed distributions of planet mass and semimajor axis. Models presented in *Ida and Lin* (2008), for example, fail to produce giant planets at all if full-strength type I migration operates. Statistically acceptable giant planet populations are reported for reductions in the efficiency of type I migration by factors of 0.01 to 0.03, with type II migration being required to form 'hot Jupiters'. With the type II time scale of $\sim 10^5$ yr being significantly shorter than disc life times, numerous giant planets migrate into the central star in these models. The survivors are planets that form late as the disc is being dispersed (through viscous evolution and photoevaporation), but just early enough to accrete appreciable gaseous envelopes. *Mordasini et al.* (2009a) and *Mordasini et al.* (2009b) present models with full-strength type I migration that are able to form a sparse population of gas giants. Cores that accrete very late in the disc life time are able to grow to large masses as they migrate because they do not exhaust their feeding zones. Type I migration of the forming planetary cores in this case, however, strongly biases the orbital radii of planetary cores to small values, leading to too many short period massive gas giants that are in contradiction of the exoplanet data.

The above studies focused primarily on forming gas giant planets, but numerous super-Earth and Neptune-mass planets have been discovered by both ground-based surveys and the Kepler mission (e.g. *Mayor et al.*, 2011; *Borucki et al.*, 2011; *Fressin et al.*, 2013). Based on 8 years of HARPS data, the former publication in this list suggests that at least 50 % of solar-type stars hosts at least one planet with a period of 100 days or less. Based on an analysis of the false-positive rate in Kepler detections, *Fressin et al.* (2013) suggest that 16.5 % of FGK stars have at least one planet between 0.8 and 1.25 $R_\oplus$ with orbital periods up to 85 days. These results appear consistent with the larger numbers of super-Earth and Neptune-like planets discovered by Kepler. In a recent study, *Howard et al.* (2010) performed a direct comparison between the predictions of population synthesis models with radial-velocity observations of extrasolar planets orbiting within 0.25 AU around 166 nearby G-, K-, and M-type stars (the η_{Earth} survey). The data indicate a high density of planets with $M_\mathrm{p} = 4$ - 10 $M_\oplus$ with periods < 10 days, in clear accord with the discoveries made by Kepler. This population is not present in the Monte-Carlo models because of rapid migration and mass growth. *Ida and Lin* (2010) recently considered specifically the formation of super-Earths using population synthesis, incorporating for the first time a treatment of planet-planet dynamical interactions. In the absence of an inner disc cavity (assumed to form by interaction with the stellar magnetic field) the simulations failed to form systems of short period super-Earths because of type I migration into the central star. This requirement for an inner disc cavity to halt inward migration, in order to explain the existence of the observed short-period planet population, appears to be a common feature in planetary formation models that include migration. Given that planets are found to have a wide-range of or-

bital radii, however, it seems unlikely that this migration stopping mechanism can apply to all systems. Given the large numbers of planets that migrate into the central star in the population synthesis models, it would appear that such a stopping mechanism when applied to all planet-forming discs would predict the existence of a significantly larger population of short-period planets than is observed. This point is illustrated by Fig. 7 which shows the mass-period relation for planets with masses $0.1 \leq M_\mathrm{p} \leq 1$ M_J in the upper panel and $10^{-3} \leq M_\mathrm{p} \leq 10^{-1}$ M_J in the lower panel. Although a clustering of giant planets between orbital periods 3-5 days is observed, there is no evidence of such a pile-up for the lower mass planets. This suggests that an inner cavity capable of stopping the migration of planets of all masses may not be a prevalent feature of planet forming discs.

N-body simulations with prescriptions for migration have been used to examine the interplay between planet growth and migration. We primarily concern ourselves here with simulations that include the early phase of oligarchic growth when a swarm of Mars-mass embryos embedded in a disc of planetesimals undergo competitive accretion. A number of studies have considered dynamical interaction between much more massive bodies in the presence of migration, but we will not consider these here. Early work included examination of the early phase of terrestrial planet formation in the presence of gas (*McNeil et al.*, 2005), which showed that even unattenuated type I migration was not inconsistent with terrestrial planet formation in discs with a moderately enhanced solids abundance. N-body simulations that explore short period super-Earth formation and demonstrate the importance of tidal interaction with the central star for disc models containing inner cavities have been presented by *Terquem and Papaloizou* (2007). *McNeil and Nelson* (2009, 2010) examined the formation of hot super-Earth and Neptune mass planets using N-body simulations combined with type I migration (full strength and with various attenuation factors). The motivation here was to examine whether or not the standard oligarchic growth picture of planet formation combined with type I migration could produce systems such as Gliese 581 and HD 69830 that contain multiple short period super-Earth and Neptune mass planets. These hot and warm super-Earth and Neptune systems probably contain up to $30 - 40$ Earth masses of rocky or icy material orbiting within 1 AU. The models incorporated a purpose-built multiple time-step scheme to allow planet formation scenarios in global disc models extending out to 15 AU to be explored. The aim was to examine whether or not hot super-Earths and Neptunes could be explained by a model of formation at large radius followed by inward migration, or whether instead smaller building blocks of terrestrial mass could migrate in and form a massive disc of embryos that accretes *in situ* to form short period bodies. As such this was a precursor study to the recent *in situ* models that neglect migration of *Hansen and Murray* (2013). The suite of some 50 simulations led to the formation of a few individual super-Earth and Neptune

mass planets, but failed to produce any systems with more than 12 Earth masses of solids interior to 1 AU.

Thommes et al. (2008) presented a suite of simulations of giant planet formation using a hybrid code in which emerging embryos were evolved using an N-body integrator combined with a 1D viscous disc model. Although unattenuated type I and type II migration were included, a number of models led to successful formation of systems of surviving gas giant planets. These models considered an initial population of planetary embryos undergoing oligarchic growth extending out to 30 AU from the star, and indicate that the right combination of planetary growth times, disc masses and life times can form surviving giant planets through the core-accretion model, provided embryos can form and grow at rather large orbital distances before migrating inward.

The role of the combined vorticity- and entropy-related corotation torque, and its ability to slow or reverse type I migration of forming planets, has not yet been explored in detail. The survival of protoplanets with masses in the range $1 \leq M_p \leq 10$ M$_\oplus$ in global 1D disc models has been studied by *Lyra et al.* (2010). These models demonstrate the existence of locations in the disc where planets of a given mass experience zero migration due to the cancellation of Lindblad and corotation torques (zero-migration radii or planetary migration traps). Planets have a tendency to migrate toward these positions, where they then sit and drift inward slowly as the gas disc disperses. Preliminary results of population synthesis calculations have been presented by *Mordasini et al.* (2011), and N-body simulations that examine the oligarchic growth scenario under the influence of strong corotation torques have been presented by *Hellary and Nelson* (2012). These studies indicate that the convergent migration that arises as planets move toward their zero-migration radii can allow a substantial increase in the rate of planetary accretion. Under conditions where the disc hosts a strongly decreasing temperature gradient, *Hellary and Nelson* (2012) computed models that led to outward migration of planetary embryos to radii ~ 50 AU, followed by gas accretion that formed gas giants at these large distances from the star. The temperature profiles required for this were substantially steeper than those that arise from calculations of passively heated discs, however, so it remains to be determined whether these conditions can ever be realised in a protoplanetary disc. Following on from the study of corotation torques experienced by planets on eccentric orbits by *Bitsch and Kley* (2010), *Hellary and Nelson* (2012) incorporated a prescription for this effect and found that planet-planet scattering causes eccentricity growth to values that effectively quench the horseshoe drag, such that crowded planetary systems during the formation epoch may continue to experience rapid inward migration. Further work is clearly required to fully assess the influence of the corotation torque on planet formation in the presence of significant planet-planet interactions.

Looking to the future, it is clear that progress in making accurate theoretical predictions that apply across the full range of observed exoplanet masses will be best achieved by bringing together the best elements of the population synthesis and N-body approaches. Some key issues that require particular attention include the structure of the disc close to the star, given its influence in shaping the short-period planet population (see section 3.1). This will require developments in both observation and theory to constrain the nature of the magnetospheric cavity and its influence on the migration of planets of all masses. Significant improvements in underlying global disc models are also required, given the sensitivity of migration processes to the detailed disc physics. Particular issues at play are the roles of magnetic fields, the thermal evolution and the nature of the turbulent flow in discs that sets the level of the effective viscous stress. These are all active areas of research at the present time and promise to improve our understanding of planet formation processes in the coming years.

4. SUMMARY POINTS

The main points to take away from this chapter are summarized below:

- Disc-planet interactions are a natural process that inevitably operates during the early evolution of planetary systems, when planets are still embedded in their protoplanetary disc. They modify all orbital elements of a planet. While eccentricity and inclination are usually damped quickly, the semi-major axis may increase or decrease more or less rapidly depending on the planet-to-star mass ratio (q) and the disc's physical properties (including its aspect ratio h).

- Planet migration comes in three main flavors. (i) Type I migration applies to low-mass planets ($\mathcal{P} \gg 1$, which is the case if $q \ll h^3$) that do not open a gap around their orbit. Its direction (inwards or outwards) and speed are very sensitive to the structure of the disc, its radiative and turbulent properties in a narrow region around the planet. While major progress in understanding the physics of type I migration has been made since PPV, robust predictions of its direction and pace will require more knowledge of protoplanetary discs in regions of planet formation. ALMA should bring precious constraints in that sense. (ii) Type II migration is for massive planets ($\mathcal{P} \lesssim 1$, or $q \geqslant q_{min}$ given by Eq. 10) that carve a deep gap around their orbit. Type II migrating planets drift inwards in a time scale comparable to or longer than the disc's viscous time scale at their orbital separation. (iii) Type III migration concerns intermediate-mass planets ($q \sim h^3$) that open a partial gap around their orbit. This very rapid, preferentially inward migration regime operates in massive discs.

- Planet-disc interaction is one major ingredient for shaping the architecture of planetary systems. The diversity of migration paths predicted for low-mass planets probably contributes to the diversity in the

mass-semi-major axis diagram of observed exoplanets. Convergent migration of several planets in a disc could provide the conditions for exciting planets eccentricity and inclination.

- The distribution of spin-orbit misalignments amongst hot Jupiters is very unlikely to have an explanation based on a single scenario for the large-scale inward migration required to bring them to their current orbital separations. Hot Jupiters on orbits aligned with their central star point preferentially to a smooth disc delivery, via type II migration, rather than to dynamical interactions with a planetary or a stellar companion, followed by star-planet tidal re-alignment.

- Convergent migration of two planets in a disc does not necessarily result in the planets being in mean-motion resonance. Turbulence in the disc, the interaction between a planet and the wake of its companion, or late star-planet tidal interactions, could explain why many multi-planet candidate systems discovered by the Kepler mission are near- or non-resonant. Wake-planet interactions could account for the observed scarcity of super-Earths on near-resonant orbits exterior to hot Jupiters.

- Recent observations of circumstellar discs have reported the existence of cavities and of large-scale vortices in millimetre-sized grains. These features do not necessarily track the presence of a giant planet in the disc. It should be kept in mind that the gaps carved by planets of around a Jupiter mass or less are narrow annuli, not cavities.

- Improving theories of planet-disc interactions in models of planet population synthesis is essential to make progress in understanding the statistical properties of exoplanets. Current discrepancies between theory and observations point to uncertainties in planet migration models as much as to uncertainties in planet mass growth, the physical properties of protoplanetary discs, or to the expected significant impact of planet-planet interactions.

REFERENCES

Adams F. C. and Bloch A. M. (2009) *Astrophys. J.*, *701*, 1381.
Adams F. C. and Laughlin G. (2003) *Icarus*, *163*, 290.
Albrecht S. et al. (2012) *Astrophys. J.*, *757*, 18.
Albrecht S. et al. (2013) *Astrophys. J.*, *771*, 11.
Alibert Y. et al. (2005) *Astron. Astrophys.*, *434*, 343.
Armitage P. J. et al. (2002) *Mon. Not. R. Astron. Soc.*, *334*, 248.

Artymowicz P. (1993a) *Astrophys. J.*, *419*, 166.
Artymowicz P. (1993b) *Astrophys. J.*, *419*, 155.
Ayliffe B. A. and Bate M. R. (2009) *Mon. Not. R. Astron. Soc.*, *397*, 657.
Ayliffe B. A. and Bate M. R. (2011) *Mon. Not. R. Astron. Soc.*, *415*, 576.
Bai X.-N. and Stone J. M. (2011) *Astrophys. J.*, *736*, 144.
Balbus S. A. and Hawley J. F. (1991) *Astrophys. J.*, *376*, 214.
Baruteau C. and Lin D. N. C. (2010) *Astrophys. J.*, *709*, 759.
Baruteau C. and Masset F. (2008a) *Astrophys. J.*, *672*, 1054.
Baruteau C. and Masset F. (2008b) *Astrophys. J.*, *678*, 483.
Baruteau C. and Masset F. (2013) in: *Lecture Notes in Physics, Berlin Springer Verlag*, vol. 861, (edited by J. Souchay, S. Mathis, and T. Tokieda), p. 201.
Baruteau C. and Papaloizou J. C. B. (2013) *Astrophys. J.*, *778*, 7.
Baruteau C. et al. (2011a) *Astron. Astrophys.*, *533*, A84.
Baruteau C. et al. (2011b) *Mon. Not. R. Astron. Soc.*, *416*, 1971.
Bate M. R. et al. (2010) *Mon. Not. R. Astron. Soc.*, *401*, 1505.
Batygin K. (2012) *Nature*, *491*, 418.
Batygin K. and Morbidelli A. (2013) *The Astronomical Journal*, *145*, 1.
Beaugé C. et al. (2012) *Research in Astronomy and Astrophysics*, *12*, 1044.
Bell K. R. et al. (1997) *Astrophys. J.*, *486*, 372.
Bitsch B. and Kley W. (2010) *Astron. Astrophys.*, *523*, A30.
Bitsch B. and Kley W. (2011) *Astron. Astrophys.*, *530*, A41.
Bitsch B. and Kley W. (2011) *Astronomy & Astrophysics*, *536*, A77.
Bitsch B. et al. (2013a) *Astron. Astrophys.*, *555*, A124.
Bitsch B. et al. (2013b) *Astron. Astrophys.*, *549*, A124.
Boley A. C. et al. (2010) *Icarus*, *207*, 509.
Borucki W. J. et al. (2011) *Astrophys. J.*, *736*, 19.
Casoli J. and Masset F. S. (2009) *Astrophys. J.*, *703*, 845.
Chambers J. E. and Wetherill G. W. (1998) *Icarus*, *136*, 304.
Chaplin W. J. et al. (2013) *Astrophys. J.*, *766*, 101.
Chatterjee S. et al. (2008) *Astrophys. J.*, *686*, 580.
Chiang E. I. and Goldreich P. (1997) *Astrophys. J.*, *490*, 368.
Cloutier R. and Lin M.-K. (2013) *Mon. Not. R. Astron. Soc.*, *434*, 621.
Correia A. C. M. et al. (2009) *Astron. Astrophys.*, *496*, 521.
Cossou C. et al. (2013) *Astron. Astrophys.*, *553*, L2.
Cresswell P. and Nelson R. P. (2006) *Astron. Astrophys.*, *450*, 833.
Cresswell P. and Nelson R. P. (2008) *Astron. Astrophys.*, *482*, 677.
Cresswell P. et al. (2007) *Astron. Astrophys.*, *473*, 329.
Crida A. (2009) *Astrophys. J.*, *698*, 606.
Crida A. and Morbidelli A. (2007) *Mon. Not. R. Astron. Soc.*, *377*, 1324.
Crida A. et al. (2006) *Icarus*, *181*, 587.
Crida A. et al. (2008) *Astron. Astrophys.*, *483*, 325.
Crida A. et al. (2009a) *Astrophys. J. Lett.*, *705*, L148.
Crida A. et al. (2009b) *Astron. Astrophys.*, *502*, 679.
D'Angelo G. and Bodenheimer P. (2013) *Astrophys. J.*, *778*, 77.
D'Angelo G. and Lubow S. H. (2008) *The Astrophysical Journal*, *685*, 560.
D'Angelo G. and Lubow S. H. (2010) *The Astrophysical Journal*, *724*, 730.
D'Angelo G. and Marzari F. (2012) *Astrophys. J.*, *757*, 50.
D'Angelo G. et al. (2003) *Astrophys. J.*, *586*, 540.
D'Angelo G. et al. (2005) *Mon. Not. R. Astron. Soc.*, *358*, 316.
Dawson R. I. and Fabrycky D. C. (2010) *The Astrophysical Journal*, *722*, 937.
Dawson R. I. and Murray-Clay R. A. (2013) *Astrophys. J. Lett.*,

767, L24.

Debes J. H. et al. (2013) *Astrophys. J.*, *771*, 45.

Desch S. J. (2007) *Astrophys. J.*, *671*, 878.

Dong R. et al. (2011) *Astrophys. J.*, *741*, 57.

Duffell P. C. and MacFadyen A. I. (2013) *The Astrophysical Journal*, *769*, 41.

Dullemond C. P. et al. (2001) *Astrophys. J.*, *560*, 957.

Dunhill A. C. et al. (2013) *Mon. Not. R. Astron. Soc.*, *428*, 3072.

Fendyke S. M. and Nelson R. P. (2014) *Mon. Not. R. Astron. Soc.*, *437*, 96.

Ferreira J. et al. (2006) *Astron. Astrophys.*, *453*, 785.

Forgan D. and Rice K. (2013) *Mon. Not. R. Astron. Soc.*, *432*, 3168.

Fouchet L. et al. (2010) *Astron. Astrophys.*, *518*, A16.

Fressin F. et al. (2013) *Astrophys. J.*, *766*, 81.

Fromang S. et al. (2005) *Mon. Not. R. Astron. Soc.*, *363*, 943.

Gammie C. F. (2001) *Astrophys. J.*, *553*, 174.

Goldreich P. and Tremaine S. (1979) *Astrophys. J.*, *233*, 857.

Goldreich P. and Tremaine S. (1980) *Astrophys. J.*, *241*, 425.

Gressel O. et al. (2011) *Mon. Not. R. Astron. Soc.*, *415*, 3291.

Gressel O. et al. (2012) *Mon. Not. R. Astron. Soc.*, *422*, 1140.

Gressel O. et al. (2013) *Astrophys. J.*, *779*, 59.

Guilet J. and Ogilvie G. I. (2012) *Mon. Not. R. Astron. Soc.*, *424*, 2097.

Guilet J. and Ogilvie G. I. (2013) *Mon. Not. R. Astron. Soc.*, *430*, 822.

Guilet J. et al. (2013) *Mon. Not. R. Astron. Soc.*, *430*, 1764.

Hansen B. M. S. and Murray N. (2013) *Astrophys. J.*, *775*, 53.

Hayashi C. (1981) *Progress of Theoretical Physics Supplement*, *70*, 35.

Hellary P. and Nelson R. P. (2012) *Mon. Not. R. Astron. Soc.*, *419*, 2737.

Howard A. W. et al. (2010) *Science*, *330*, 653.

Ida S. and Lin D. N. C. (2004) *Astrophys. J.*, *604*, 388.

Ida S. and Lin D. N. C. (2008) *Astrophys. J.*, *673*, 487.

Ida S. and Lin D. N. C. (2010) *Astrophys. J.*, *719*, 810.

Johnson E. T. et al. (2006) *Astrophys. J.*, *647*, 1413.

Jurić M. and Tremaine S. (2008) *Astrophys. J.*, *686*, 603.

Ketchum J. A. et al. (2011) *The Astrophysical Journal*, *726*, 53.

Kley W. and Crida A. (2008) *Astron. Astrophys.*, *487*, L9.

Kley W. and Nelson R. P. (2012) *Annu. Rev. Astron. Astrophys.*, *50*, 211.

Kley W. et al. (2004) *Astron. Astrophys.*, *414*, 735.

Kley W. et al. (2005) *Astron. Astrophys.*, *437*, 727.

Kley W. et al. (2009) *Astron. Astrophys.*, *506*, 971.

Korycansky D. G. and Papaloizou J. C. B. (1996) *Astrophys. J. Suppl.*, *105*, 181.

Korycansky D. G. and Pollack J. B. (1993) *Icarus*, *102*, 150.

Kretke K. A. and Lin D. N. C. (2012) *The Astrophysical Journal*, *755*, 74.

Kunz M. W. and Lesur G. (2013) *Mon. Not. R. Astron. Soc.*, *434*, 2295.

Lagrange A. et al. (2010) *Science*, *329*, 57.

Lai D. et al. (2011) *Mon. Not. R. Astron. Soc.*, *412*, 2790.

Laughlin G. et al. (2004) *Astrophys. J.*, *608*, 489.

Lee M. H. and Peale S. J. (2002) *Astrophys. J.*, *567*, 596.

Lega E. et al. (2013) *Mon. Not. R. Astron. Soc.*, *431*, 3494.

Li H. et al. (2000) *Astrophys. J.*, *533*, 1023.

Libert A.-S. and Tsiganis K. (2009) *Mon. Not. R. Astron. Soc.*, *400*, 1373.

Libert A.-S. and Tsiganis K. (2011) *Celestial Mechanics and Dynamical Astronomy*, *111*, 201.

Lin D. N. C. and Papaloizou J. (1979) *Mon. Not. R. Astron. Soc.*, *186*, 799.

Lin D. N. C. and Papaloizou J. (1986a) *Astrophys. J.*, *307*, 395.

Lin D. N. C. and Papaloizou J. (1986b) *Astrophys. J.*, *309*, 846.

Lin M.-K. and Papaloizou J. C. B. (2010) *Mon. Not. R. Astron. Soc.*, *405*, 1473.

Lin M.-K. and Papaloizou J. C. B. (2012) *Mon. Not. R. Astron. Soc.*, *421*, 780.

Lissauer J. J. et al. (2011a) *Nature*, *470*, 53.

Lissauer J. J. et al. (2011b) *Astrophys. J. Suppl.*, *197*, 8.

Lithwick Y. and Wu Y. (2012) *The Astrophysical Journal Letters*, *756*, L11.

Lovelace R. V. E. et al. (1999) *Astrophys. J.*, *513*, 805.

Lubow S. H. (1991) *Astrophys. J.*, *381*, 259.

Lyra W. et al. (2010) *Astrophys. J. Lett.*, *715*, L68.

Machida M. N. et al. (2010) *Mon. Not. R. Astron. Soc.*, *405*, 1227.

Marcy G. W. and Butler R. P. (1995) in: *American Astronomical Society Meeting Abstracts*, vol. 27 of *Bulletin of the American Astronomical Society*, p. 1379.

Marois C. et al. (2010) *Nature*, *468*, 1080.

Marzari F. et al. (2010) *Astron. Astrophys.*, *514*, L4.

Masset F. and Snellgrove M. (2001) *Mon. Not. R. Astron. Soc.*, *320*, L55+.

Masset F. S. (2001) *Astrophys. J.*, *558*, 453.

Masset F. S. (2002) *Astron. Astrophys.*, *387*, 605.

Masset F. S. (2008) *EAS Publ. Series*, pp. 165–244.

Masset F. S. (2011) *Celestial Mechanics and Dynamical Astronomy*, *111*, 131.

Masset F. S. and Casoli J. (2009) *Astrophys. J.*, *703*, 857.

Masset F. S. and Casoli J. (2010) *Astrophys. J.*, *723*, 1393.

Masset F. S. and Papaloizou J. C. B. (2003) *Astrophys. J.*, *588*, 494.

Masset F. S. et al. (2006) *Astrophys. J.*, *652*, 730.

Matsumura S. et al. (2010) *Astrophys. J.*, *714*, 194.

Mayor M. and Queloz D. (1995) *Nature*, *378*, 355.

Mayor M. et al. (2011) *ArXiv e-prints*.

McNeil D. et al. (2005) *Astron. J.*, *130*, 2884.

McNeil D. S. and Nelson R. P. (2009) *Mon. Not. R. Astron. Soc.*, *392*, 537.

McNeil D. S. and Nelson R. P. (2010) *Mon. Not. R. Astron. Soc.*, *401*, 1691.

Migaszewski C. et al. (2012) *Mon. Not. R. Astron. Soc.*, *427*, 770.

Moeckel N. and Armitage P. J. (2012) *Mon. Not. R. Astron. Soc.*, *419*, 366.

Morbidelli A. and Crida A. (2007) *Icarus*, *191*, 158.

Morbidelli A. et al. (2007) *Astron. J.*, *134*, 1790.

Mordasini C. et al. (2009a) *Astron. Astrophys.*, *501*, 1139.

Mordasini C. et al. (2009b) *Astron. Astrophys.*, *501*, 1161.

Mordasini C. et al. (2011) in: *IAU Symposium*, vol. 276 of *IAU Symposium*, (edited by A. Sozzetti, M. G. Lattanzi, & A. P. Boss), pp. 72–75.

Mordasini C. et al. (2012) *Astron. Astrophys.*, *547*, A112.

Müller T. W. A. et al. (2012) *Astron. Astrophys.*, *541*, A123.

Mustill A. J. and Wyatt M. C. (2011) *Mon. Not. R. Astron. Soc.*, *413*, 554.

Muto T. et al. (2008) *Astrophys. J.*, *679*, 813.

Muto T. et al. (2010) *Astrophys. J.*, *724*, 448.

Muto T. et al. (2011) *Astrophys. J.*, *737*, 37.

Nayakshin S. (2010) *Mon. Not. R. Astron. Soc.*, *408*, L36.

Nelson R. P. (2005) *Astron. Astrophys.*, *443*, 1067.

Nelson R. P. and Gressel O. (2010) *Mon. Not. R. Astron. Soc.*, *409*, 639.

Nelson R. P. and Papaloizou J. C. B. (2002) *Mon. Not. R. Astron. Soc.*, *333*, L26.

Nelson R. P. and Papaloizou J. C. B. (2004) *Mon. Not. R. Astron. Soc.*, *350*, 849.

Ogilvie G. I. and Lubow S. H. (2002) *Mon. Not. R. Astron. Soc.*, *330*, 950.

Oishi J. S. et al. (2007) *Astrophys. J.*, *670*, 805.

Olofsson J. et al. (2012) *Astron. Astrophys.*, *542*, A90.

Ormel C. W. and Klahr H. H. (2010) *Astron. Astrophys.*, *520*, A43.

Paardekooper S.-J. (2012) *Mon. Not. R. Astron. Soc.*, *421*, 3286.

Paardekooper S.-J. and Mellema G. (2006) *Astron. Astrophys.*, *459*, L17.

Paardekooper S.-J. and Mellema G. (2008) *Astron. Astrophys.*, *478*, 245.

Paardekooper S.-J. and Papaloizou J. C. B. (2008) *Astron. Astrophys.*, *485*, 877.

Paardekooper S.-J. and Papaloizou J. C. B. (2009a) *Mon. Not. R. Astron. Soc.*, *394*, 2283.

Paardekooper S.-J. and Papaloizou J. C. B. (2009b) *Mon. Not. R. Astron. Soc.*, *394*, 2297.

Paardekooper S.-J. et al. (2010) *Mon. Not. R. Astron. Soc.*, *401*, 1950.

Paardekooper S.-J. et al. (2011) *Mon. Not. R. Astron. Soc.*, *410*, 293.

Paardekooper S.-J. et al. (2013) *Mon. Not. R. Astron. Soc.*, *434*, 3018.

Papaloizou J. C. B. (2011) *Celestial Mechanics and Dynamical Astronomy*, *111*, 83.

Papaloizou J. C. B. and Larwood J. D. (2000) *Mon. Not. R. Astron. Soc.*, *315*, 823.

Papaloizou J. C. B. and Szuszkiewicz E. (2005) *Mon. Not. R. Astron. Soc.*, *363*, 153.

Papaloizou J. C. B. and Terquem C. (2006) *Reports on Progress in Physics*, *69*, 119.

Papaloizou J. C. B. et al. (2001) *Astron. Astrophys.*, *366*, 263.

Papaloizou J. C. B. et al. (2004) *Mon. Not. R. Astron. Soc.*, *350*, 829.

Papaloizou J. C. B. et al. (2007) *Protostars and Planets V*, pp. 655–668.

Pepliński A. et al. (2008a) *Mon. Not. R. Astron. Soc.*, *386*, 164.

Pepliński A. et al. (2008b) *Mon. Not. R. Astron. Soc.*, *387*, 1063.

Pierens A. and Huré J.-M. (2005) *Astron. Astrophys.*, *433*, L37.

Pierens A. and Nelson R. P. (2008) *Astron. Astrophys.*, *482*, 333.

Pierens A. et al. (2011) *Astron. Astrophys.*, *531*, A5.

Pierens A. et al. (2012) *Mon. Not. R. Astron. Soc.*, *427*, 1562.

Podlewska-Gaca E. et al. (2012) *Mon. Not. R. Astron. Soc.*, *421*, 1736.

Pollack J. B. et al. (1996) *Icarus*, *124*, 62.

Quanz S. P. et al. (2013) *Astrophys. J. Lett.*, *766*, L2.

Quillen A. C. (2006) *Mon. Not. R. Astron. Soc.*, *365*, 1367.

Rafikov R. R. (2002) *The Astrophysical Journal*, *572*, 566.

Rafikov R. R. (2005) *Astrophys. J. Lett.*, *621*, L69.

Rein H. (2012a) *Mon. Not. R. Astron. Soc.*, *427*, L21.

Rein H. (2012b) *Mon. Not. R. Astron. Soc.*, *422*, 3611.

Rein H. et al. (2010) *Astron. Astrophys.*, *510*, A4.

Rivier G. et al. (2012) *Astron. Astrophys.*, *548*, A116.

Rogers T. M. and Lin D. N. C. (2013) *Astrophys. J. Lett.*, *769*, L10.

Rogers T. M. et al. (2012) *Astrophys. J. Lett.*, *758*, L6.

Sanchis-Ojeda R. et al. (2012) *Nature*, *487*, 449.

Simon J. B. et al. (2013) *Astrophys. J.*, *775*, 73.

Snellgrove M. D. et al. (2001) *Astron. Astrophys.*, *374*, 1092.

Steffen J. H. et al. (2013) *Mon. Not. R. Astron. Soc.*, *428*, 1077.

Szuszkiewicz E. and Podlewska-Gaca E. (2012) *Origins of Life and Evolution of the Biosphere*, *42*, 113.

Takeda G. and Rasio F. A. (2005) *Astrophys. J.*, *627*, 1001.

Tanaka H. and Ward W. R. (2004) *Astrophys. J.*, *602*, 388.

Tanaka H. et al. (2002) *Astrophys. J.*, *565*, 1257.

Tanigawa T. et al. (2012) *Astrophys. J.*, *747*, 47.

Terquem C. and Papaloizou J. C. B. (2007) *Astrophys. J.*, *654*, 1110.

Terquem C. E. J. M. L. J. (2003) *Mon. Not. R. Astron. Soc.*, *341*, 1157.

Teyssandier J. et al. (2013) *Mon. Not. R. Astron. Soc.*, *428*, 658.

Thommes E. W. et al. (2008) *Science*, *321*, 814.

Triaud A. H. M. J. et al. (2010) *Astron. Astrophys.*, *524*, A25.

Tsiganis K. et al. (2005) *Nature*, *435*, 459.

Uribe A. L. et al. (2011) *Astrophys. J.*, *736*, 85.

Uribe A. L. et al. (2013) *Astrophys. J.*, *769*, 97.

Varnière P. et al. (2004) *Astrophys. J.*, *612*, 1152.

Vorobyov E. I. (2013) *Astron. Astrophys.*, *552*, A129.

Walsh K. J. et al. (2011) *Nature*, *475*, 206.

Ward W. R. (1991) in: *Lunar and Planetary Institute Science Conference Abstracts*, vol. 22 of *Lunar and Planetary Inst. Technical Report*, p. 1463.

Ward W. R. (1997) *Icarus*, *126*, 261.

Xiang-Gruess M. and Papaloizou J. C. B. (2013) *Mon. Not. R. Astron. Soc.*, *431*, 1320.

Zhu Z. et al. (2012a) *Astrophys. J.*, *746*, 110.

Zhu Z. et al. (2012b) *Astrophys. J.*, *755*, 6.

Zhu Z. et al. (2013) *Astrophys. J.*, *768*, 143.